nature medicine

Fetuin-A acts as an endogenous ligand of TLR4 to promote lipid-induced insulin resistance

Durba Pal[1,7], Suman Dasgupta[1,2,7], Rakesh Kundu[1], Sudipta Maitra[1], Gobardhan Das[3], Satinath Mukhopadhyay[4], Sukanta Ray[5], Subeer S Majumdar[6] & Samir Bhattacharya[1,2]

Toll-like receptor 4 (TLR4) has a key role in innate immunity by activating an inflammatory signaling pathway. Free fatty acids (FFAs) stimulate adipose tissue inflammation through the TLR4 pathway, resulting in insulin resistance[1–7]. However, current evidence suggests that FFAs do not directly bind to TLR4[8,9], but an endogenous ligand for TLR4 remains to be identified. Here we show that fetuin-A (FetA) could be this endogenous ligand and that it has a crucial role in regulating insulin sensitivity via Tlr4 signaling in mice. *FetA* (officially known as *Ahsg*) knockdown in mice with insulin resistance caused by a high-fat diet (HFD) resulted in downregulation of Tlr4-mediated inflammatory signaling in adipose tissue, whereas selective administration of FetA induced inflammatory signaling and insulin resistance. FFA-induced proinflammatory cytokine expression in adipocytes occurred only in the presence of both FetA and Tlr4; removing either of them prevented FFA-induced insulin resistance. We further found that FetA, through its terminal galactoside moiety, directly binds the residues of Leu100–Gly123 and Thr493–Thr516 in Tlr4. FFAs did not produce insulin resistance in adipocytes with mutated Tlr4 or galactoside-cleaved FetA. Taken together, our results suggest that FetA fulfills the requirement of an endogenous ligand for TLR4 through which lipids induce insulin resistance. This may position FetA as a new therapeutic target for managing insulin resistance and type 2 diabetes.

Insulin resistance is one of the major outcomes of chronic inflammation fueled by FFAs[10–13]. There has been growing evidence over the last few years that FFA-induced production of proinflammatory cytokines from inflamed adipose tissue is mediated through TLR4, a pattern recognition receptor. FFA-mediated activation of the TLR4 and nuclear factor-κB (NF-κB) pathways has been increasingly recognized as a cause of insulin resistance[4–8]; however, in the absence of a direct association between FFAs and the TLR4-MD2 complex[8,9], how FFAs activate TLR4 signaling remains unresolved. This has created a crucial deficiency in the understanding of the regulation of the FFA-TLR4 signaling pathway. Identification of an endogenous ligand that allows FFA-TLR4 crosstalk is therefore crucial to our understanding of the mechanism by which FFAs induce insulin resistance.

FetA, a liver secretory glycoprotein, stimulates the production of inflammatory cytokines from adipocytes and macrophages and therefore acts as a biomarker of chronic inflammatory diseases[14–16]. We have demonstrated that FFAs cause FetA overexpression through NF-κB[17] and that elevation of FetA's circulatory level enhanced proinflammatory cytokine production from adipocytes[17,18]. Notably, *FetA*- or *Tlr4*-knockout mice are protected from HFD-induced insulin resistance[4,19–21] and it has also been reported that FetA acts as a major carrier protein of FFAs in the circulation[22]. On the basis of these reports, we hypothesized that FetA may present FFAs to TLR4 by its actions as an endogenous ligand for this receptor.

To examine our hypothesis, we determined FetA concentration in serum, as well as *TLR4, IL-6* and *TNF-α* expression and NF-κB activation in adipocytes, isolated from obese diabetic human subjects, HFD-induced insulin resistant mice and dyslipidemic *db/db* mice. We found that all of these parameters were significantly elevated in these conditions in comparison with nonobese nondiabetic human subjects, standard diet (SD)-fed BALB/c mice and wild-type BL/6 mice, respectively (**Fig. 1a** and **Supplementary Fig. 1a**). This suggests an association between lipid, FetA concentration and TLR4 expression and activation in states of insulin resistance.

As $FetA^{-/-}$ and $Tlr4^{-/-}$ mice are protected from lipid-induced insulin resistance[4,19–21], we thought that using them to examine FetA-TLR4 interdependence in producing insulin resistance might not be useful. We therefore prepared diet-induced insulin-resistant mice and then used vivo-morpholino (VMO)-based gene knockdown of *FetA* or *Tlr4* ($FetA^{KD}$ or $Tlr4^{KD}$ mice; we verified knockdown efficiency by real-time quantitative PCR (qPCR), but knockdown did not significantly alter body and adipose tissue weight) (**Supplementary Fig. 1b**,**c**), as this would be an ideal model to understand the FetA-Tlr4 association in implementing insulin resistance. $FetA^{KD}$ or $Tlr4^{KD}$ mice were protected from insulin resistance due to a HFD, as was evident from differences in blood glucose levels, [^{14}C]-2-deoxy-D-glucose ([^{14}C]-2DOG) uptake, responses to

[1]Cellular and Molecular Endocrinology Laboratory, Centre for Advanced Studies in Zoology, School of Life Science, Visva-Bharati (A Central University), Santiniketan, West Bengal, India. [2]Council of Scientific and Industrial Research (CSIR)–North-East Institute of Science and Technology (NEIST), Jorhat, India. [3]Immunology Group, International Centre for Genetic Engineering and Biotechnology, New Delhi, India. [4]Department of Endocrinology & Metabolism, Institute of Post-Graduate Medical Education & Research-Seth Sukhlal Karnani Memorial Hospital (IPGME&R-SSKM) Hospital, Kolkata, India. [5]Division of Surgical Gastroenterology, IPGME&R-SSKM Hospital, Kolkata, India. [6]Division of Cellular Endocrinology, National Institute of Immunology, New Delhi, India. [7]These authors contributed equally to this work. Correspondence should be addressed to S.B. (bhattacharyasa@gmail.com).

Received 1 March; accepted 31 May; published online 29 July 2012; doi:10.1038/nm.2851

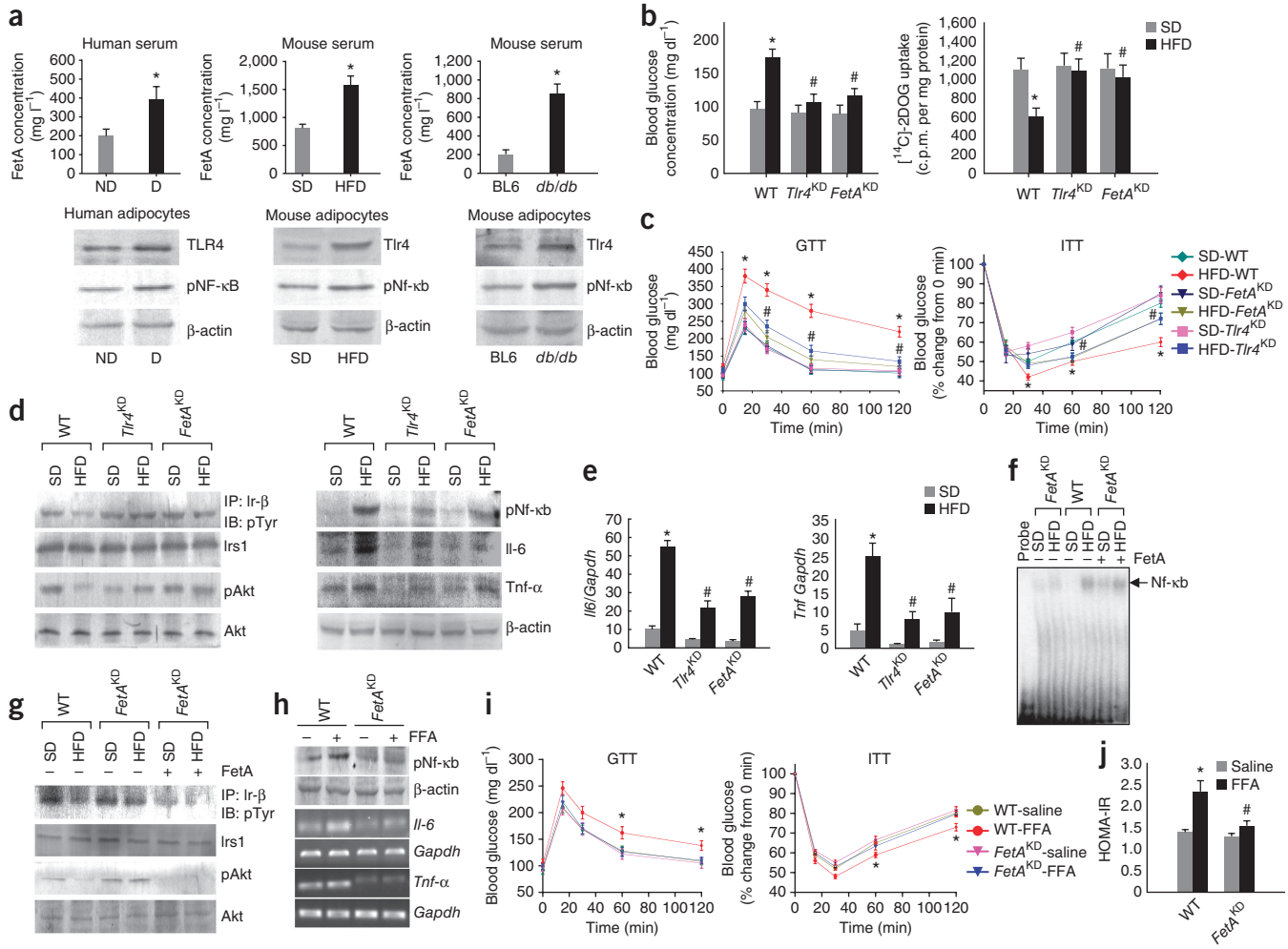

Figure 1 FetA effect on lipid-induced TLR4 activation in adipocytes. (**a**) ELISA of serum FetA (top) and western blot of TLR4 and pNF-κB level (bottom) in the adipose tissue of human subjects without diabetes (ND, $n = 12$) or with diabetes (D, $n = 10$); standard-diet (SD)- or HFD-fed mice ($n = 6$); and BL6 or *db/db* mice; ($n = 5$). $^{*}P < 0.01$ versus ND, SD or BL6. Parameters for insulin resistance was determined in SD- or HFD-fed WT or *Tlr4*^{KD} or *FetA*^{KD} mice. (**b**) Blood glucose concentration (left) and [^{14}C]-2DOG uptake by skeletal muscle cells (right). (**c**) Glucose tolerance test (GTT, left) and insulin tolerance test (ITT, right) $^{*}P < 0.01$ versus SD-WT; $^{\#}P < 0.05$ versus HFD-WT. (**d**) Western blot showing phosphorylation status of insulin receptor β (Ir-β) and Akt (left) along with pNf-κb, Il-6 and Tnf-α abundance (right). IP; immunoprecipitation; IB; immunoblot. (**e**) Quantification of *Il-6* and *Tnf-α* mRNA expression in adipose tissue of the above-mentioned mice, $^{*}P < 0.001$ versus SD-WT; $^{\#}P < 0.01$ versus HFD-WT. (**f**,**g**) Electrophoretic mobility shift assay demonstrating Nf-κb binding to DNA (**f**) and western blot showing pIr-β and pAkt abundance (**g**) in the adipose tissue from SD-*FetA*^{KD} and HFD-*FetA*^{KD} mice in response to FetA. (**h**) Western blot of pNf-κb and RT-PCR of *Il-6* and *Tnf-α* in the adipose tissue of saline- or FFA-infused WT and *FetA*^{KD} mice ($n = 5$). β-actin or Irs1 or Akt or *Gapdh* was used as loading control. (**i**) GTT and ITT in saline- or FFA-infused WT and *FetA*^{KD} mice ($n = 5$), $^{*}P < 0.05$ versus *FetA*^{KD}-FFA. (**j**) HOMA-IR in saline- or FFA-infused WT and *FetA*^{KD} mice ($n = 5$). $^{*}P < 0.05$ versus WT-saline; $^{\#}P < 0.05$ versus WT-FFA. Data represent means ± s.e.m.

a glucose tolerance test (GTT) and an insulin tolerance test (ITT), homeostasis model assessment–insulin resistance (HOMA-IR) scores and phosphorylation of the insulin-signaling molecules insulin receptor-β (Ir-β) and Akt (**Fig. 1b–d** and **Supplementary Fig. 1d**), suggesting that both FetA and Tlr4 are necessary for lipid-mediated insulin resistance in our mouse model. This was further indicated by the reduced Nf-κb activity along with the marked reduction of interleukin-6 (*Il-6*) and tumor necrosis factor-α (*Tnf-α*) mRNA expression in adipocytes from *FetA*^{KD} and *Tlr4*^{KD} mice as compared to wild-type mice under the same dietary regimen. (**Fig. 1e**).

The involvement of TLR4 in lipid-induced insulin resistance has been shown previously[4–7], therefore it was expected, but we were intrigued by the similar trend of the results in *FetA*^{KD} mice. Thus, to validate our findings further, we introduced FetA, free of endotoxin (a TLR4 ligand expressed by bacteria and hence a common contaminant in recombinant proteins isolated from bacterial expression systems) (**Supplementary Fig. 1e–h**) to *FetA*^{KD} mice and found this manipulation resulted in lipid-induced insulin resistance (**Fig. 1f,g** and **Supplementary Fig. 1d**).

As the liver is a major source of FetA, we partially hepatectomized rats to lower the serum levels of FetA as an alternative means to genetically knocking down the expression of the protein. We observed a significant decrease in serum FetA levels along with a reduction in pNf-κb, Il-6 and Tnf-α in partially hepatectomized HFD rats as compared to control HFD rats (**Supplementary Fig. 1i**).

Adipose tissue from lipid-infused *FetA*^{KD} mice did not show Tlr4 activation, whereas it was apparent in wild-type (WT) mice (**Fig. 1h**). Glucose and insulin tolerances were decreased, and

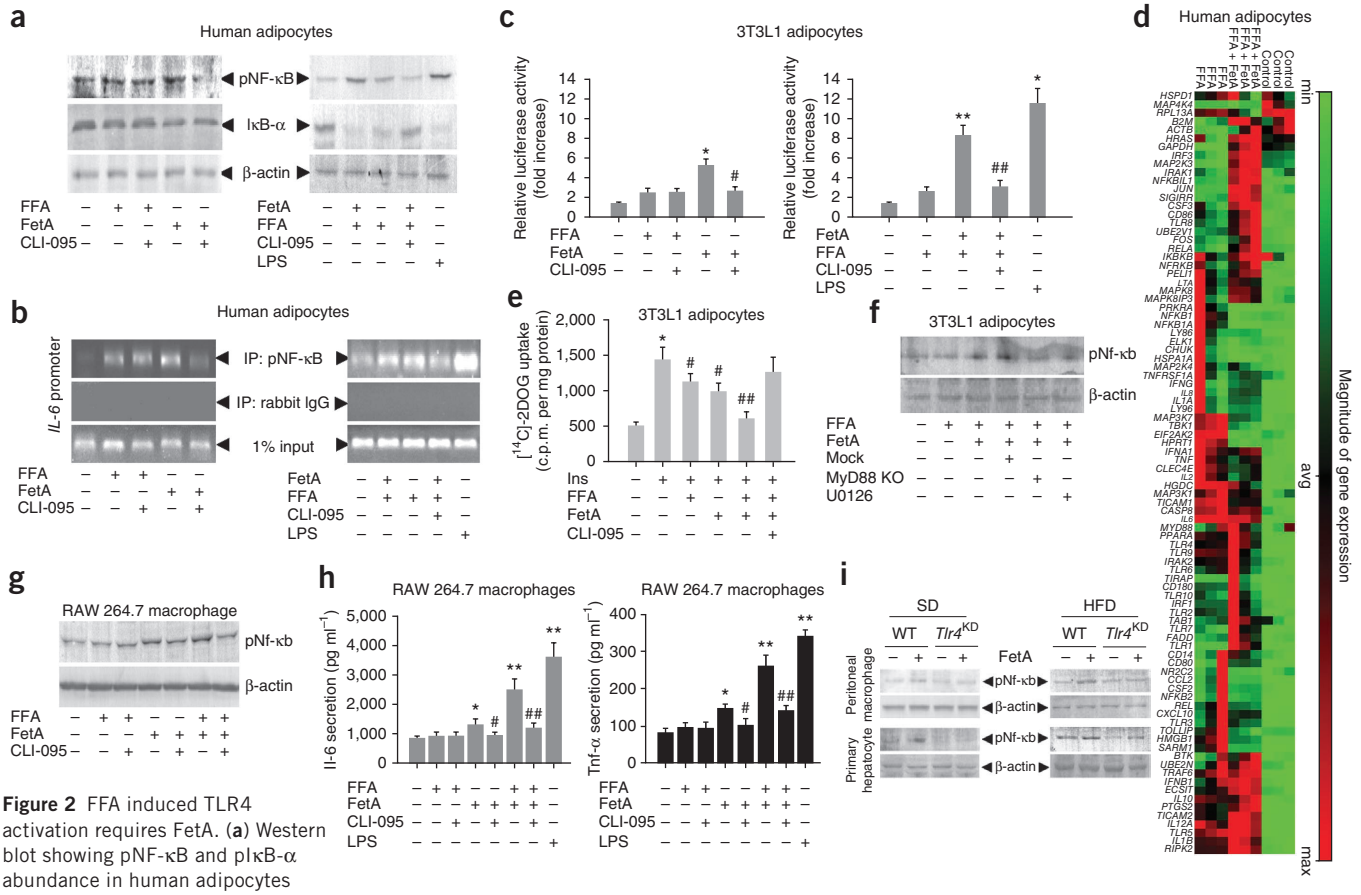

Figure 2 FFA induced TLR4 activation requires FetA. (**a**) Western blot showing pNF-κB and pIκB-α abundance in human adipocytes incubated with FFA or FetA (left) or FFA or FFA + FetA (right) in the absence or presence of CLI-095. Lipopolysaccharide (LPS) was used as positive control. (**b**,**c**) ChIP assay showing Nf-κb binding to an *Il-6* promoter in human adipocytes (**b**) and the determination of relative luciferase activity in 3T3L1 adipocytes (**c**) after the incubation of FFA or FetA (left panel) or FFA or FFA + FetA (right panel) in the absence or presence of CLI-095. $^{*}P < 0.01$, $^{**}P < 0.001$ versus Control (–); $^{\#}P < 0.01$ versus FetA, $^{\#\#}P < 0.001$ versus FFA + FetA. (**d**) PCR array showing the gene expression of TLR4 pathway components in human adipocytes treated without (control) or with FFA or FFA + FetA. (**e**) [^{14}C]-2DOG uptake by 3T3L1 adipocytes in response to the indicated conditions. $^{*}P < 0.001$ versus Control (–); $^{\#}P < 0.05$ versus insulin (Ins); $^{\#\#}P < 0.01$ versus Ins. (**f**) Western blot of pNf-κb level in MyD88-knockout (KO) or U0126-incubated 3T3L1 adipocytes. (**g**) Western blots showing pNf-κb level in macrophage cells incubated under the indicated conditions. (**h**) ELISA showing Il-6 (left) and Tnf-α (right) secretion from the macrophages. $^{*}P < 0.05$, $^{**}P < 0.001$ versus Control (–); $^{\#}P < 0.05$ versus FetA, $^{\#\#}P < 0.001$ versus FFA + FetA. (**i**) Western blots showing pNf-κb level in peritoneal macrophages and primary hepatocytes obtained from SD- or HFD-fed WT and *Tlr4*^{KD} mice without or with FetA incubation. Values are means ± s.e.m.

insulin resistance was increased after palmitate infusion in WT mice, whereas in *FetA*^{KD} mice these parameters were unchanged (**Fig. 1i**,**j** and **Supplementary Fig. 1j**).

These results implicate three important possibilities regarding the involvement of FetA and Tlr4 in lipid-induced insulin resistance: (i) the decrease in Nf-κb phosphorylation in the absence of FetA may be due to impaired Tlr4 signaling, (ii) insulin resistance due to lipotoxicity requires the presence of both Tlr4 and FetA, and (iii) a physical association between FFAs, FetA and Tlr4 is likely to be linked to insulin resistance.

To address the first possibility, we investigated whether FFA-induced Tlr4 signaling requires FetA. Palmitate (a FFA) had maximum binding to FetA and produced the highest inflammatory response in 3T3L1 mouse adipocytes as compared to other FFAs (**Supplementary Fig. 2a**,**b**). We therefore incubated human adipocytes or 3T3L1 cells with palmitate or FetA or both of them in the absence or presence of CLI-095, a TLR4 signaling inhibitor, followed by the determination of NF-κB activity through western blotting, chromatin immunoprecipitation (ChIP) and reporter assays. FFA-induced activation of NF-κB and elevated expression of the cytokines *IL-6* and *TNF-α* occurred only in the presence of FetA, whereas CLI-095 incubation or silencing of Tlr4 expression by siRNA prevented this activation and cytokine expression (**Fig. 2a**–**c** and **Supplementary Fig. 2c**,**d**).

These results were notable given previous reports suggesting that FFAs activate the Tlr4 signaling pathway in 3T3L1 adipocytes[2,4,6,23,24]. One possibility for this disparity could be the high FetA concentration in FBS[25]. As commercially available FBS contains ~20 mg ml^{-1} FetA, conventionally used culture media (with 10% FBS) have a substantial amount of FetA, which might allow exogenously added FFAs to induce Tlr4 activation. We therefore used serum-free medium in our experiments. FFAs alone had a marginal stimulatory effect that seemed to be independent of Tlr4 because addition of CLI-095 to the medium did not alter the response to exogenous FFAs (**Fig. 2a**–**c**). That FFA can induce inflammatory signaling pathways independent of Tlr4 influence has also been shown by others[26,27]. In contrast, stimulation of Nf-κb activation by FetA was inhibited by CLI-095, indicating that FetA's effect is mediated through Tlr4 (**Fig. 2a**–**c**).

We made similar observations when we incubated macrophages and adipocytes obtained from *Tlr4*$^{-/-}$ mice (Tlr4 knockout was verified by RT-PCR, **Supplementary Fig. 2e**) with FetA and saw that FetA did

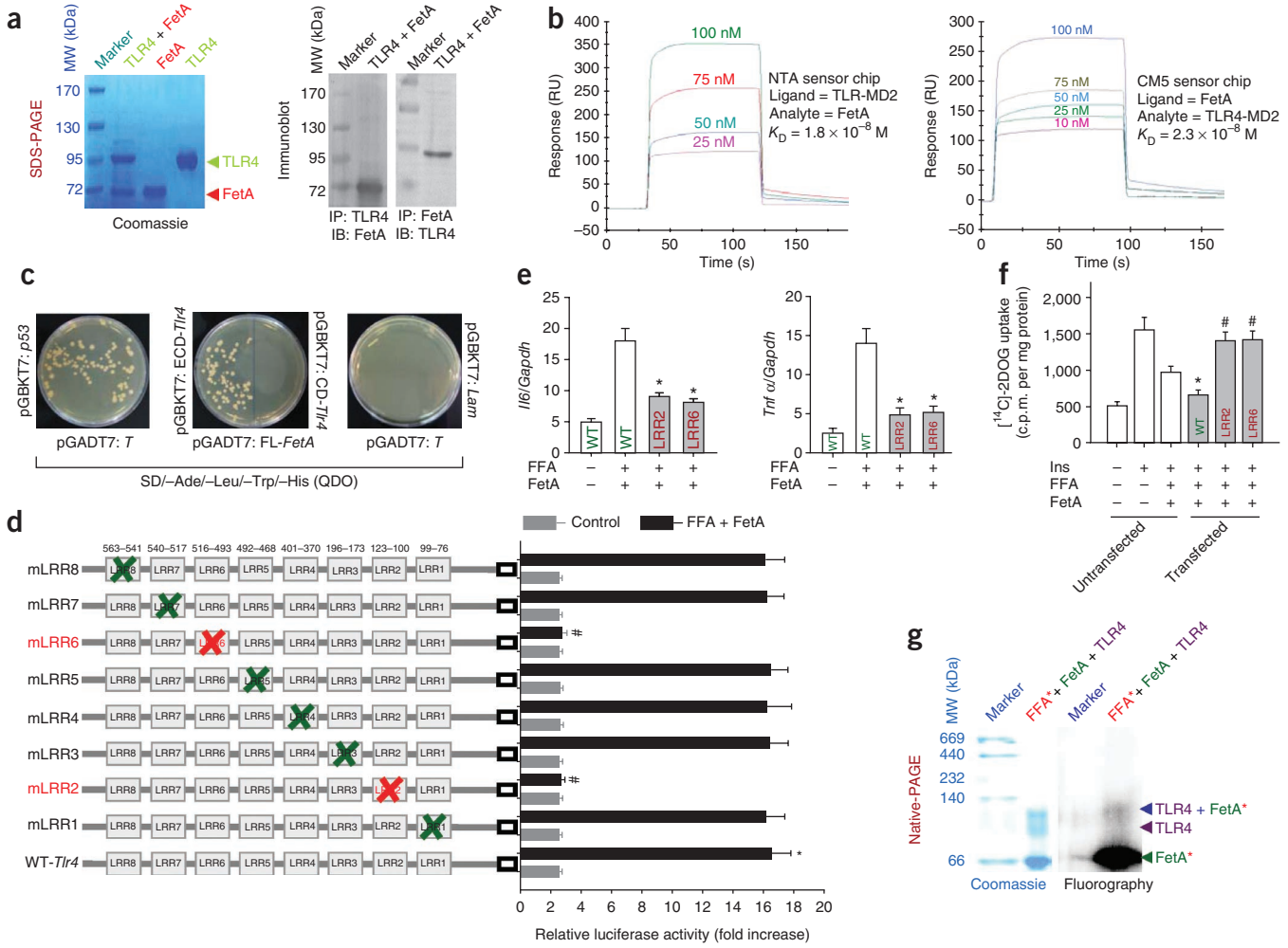

Figure 3 FetA-TLR4 interaction induces proinflammatory cytokine expression and insulin resistance in adipocytes. (**a**) SDS-PAGE (left) and western blot (right) of coimmunoprecipitation study demonstrating FetA binding to TLR4. (**b**) SPR study showing representative sensorgrams obtained from flowing of the indicated concentrations of FetA (left) or TLR4-MD2 (right) over the TLR4-MD2 immobilized NTA sensor chip or FetA immobilized CM5 sensor chip, respectively. Sensorgrams are represented as response units (RU) at specified time (s). (**c**) Y2H showing FetA binding with the extracellular domain (ECD) of *Tlr4* as indicated by the growth colonies in growth-limiting plates. pGADT7-*t* and pGBKT7-*p53* plasmids and pGADT7-*t* and pGBKT7-*Lam* plasmids were used as positive and negative controls, respectively. (**d**) Schematic structure showing the eight predicted LRR regions in the ECD of Tlr4. These were individually mutated by site-directed mutagenesis (left), and transfected 3T3L1 adipocytes were examined for *Nf-κb* luciferase activity (right). $^*P < 0.001$ versus control (–); $^{\#}P < 0.001$ versus WT *Tlr4*. (**e**) Quantification of *Il-6* and *Tnf-α* mRNA expression. $^*P < 0.01$ versus WT *Tlr4*. (**f**) [^{14}C]-2DOG uptake in WT, LRR2-mutated and LRR6-mutated *Tlr4*–transfected 3T3L1 adipocytes. $^*P < 0.05$ versus WT *Tlr4* untransfected; $^{\#}P < 0.01$ versus WT *Tlr4* transfected. (**g**) Representative gels of native-PAGE and its fluorography showing formation of a ternary complex between FFA, FetA and TLR4 (asterisks represent [^{3}H]-palmitate and its association with FetA). Data represent means ± s.e.m.

not activate the Tlr4 pathway, thus indicating the requirement of Tlr4 for FetA's effect on Nf-κb activation (**Supplementary Fig. 2f**). We also evaluated FFA plus FetA (FFA+FetA) induction of TLR4 signaling by PCR array and found that gene expression of various proinflammatory cytokines in human adipocytes belonging to the TLR4 pathway were greatly upregulated, whereas FFA alone produced a marginal effect (**Fig. 2d**). This was also reflected in the insulin sensitivity assay, wherein FFA+FetA showed a significantly greater inhibitory effect on insulin-stimulated [^{14}C]-2DOG uptake by 3T3L1 adipocytes as compared to FFA or FetA alone (**Fig. 2e**).

Because myeloid differentiation primary response gene 88 (MyD88) and mitogen-activated protein kinase kinase (MEK) are downstream of the TLR4 signaling pathway[28,29], failure of Nf-κb activation in MyD88-knockout 3T3L1 adipocyte cells incubated with FFA+FetA or in cells preincubated with the MEK inhibitor U0126 (**Fig. 2f**) suggest that FFA+FetA acts through the Tlr4 pathway. We found that FFA+FetA experiments with macrophages also had similar results; FFA augmentation of Tlr4 activation was dependent on FetA (**Fig. 2g,h**), as observed with adipocytes, indicating a link between insulin resistance and innate immunity with FFAs as reported earlier[4]. We examined this further in primary cell cultures of macrophage and hepatocytes obtained from standard diet–fed *Tlr4*^{KD} mice, in which FetA alone failed to induce Nf-κb activation but did so in standard diet–fed WT mice (**Fig. 2i**). We obtained similar results with HFD-fed insulin-resistant mice (**Fig. 2i**), suggesting that Tlr4 is necessary to produce the FFA+FetA effect on Nf-κb activation.

From these results it would seem evident that FetA is required for FFA-TLR4 signaling. However, we along with others have observed

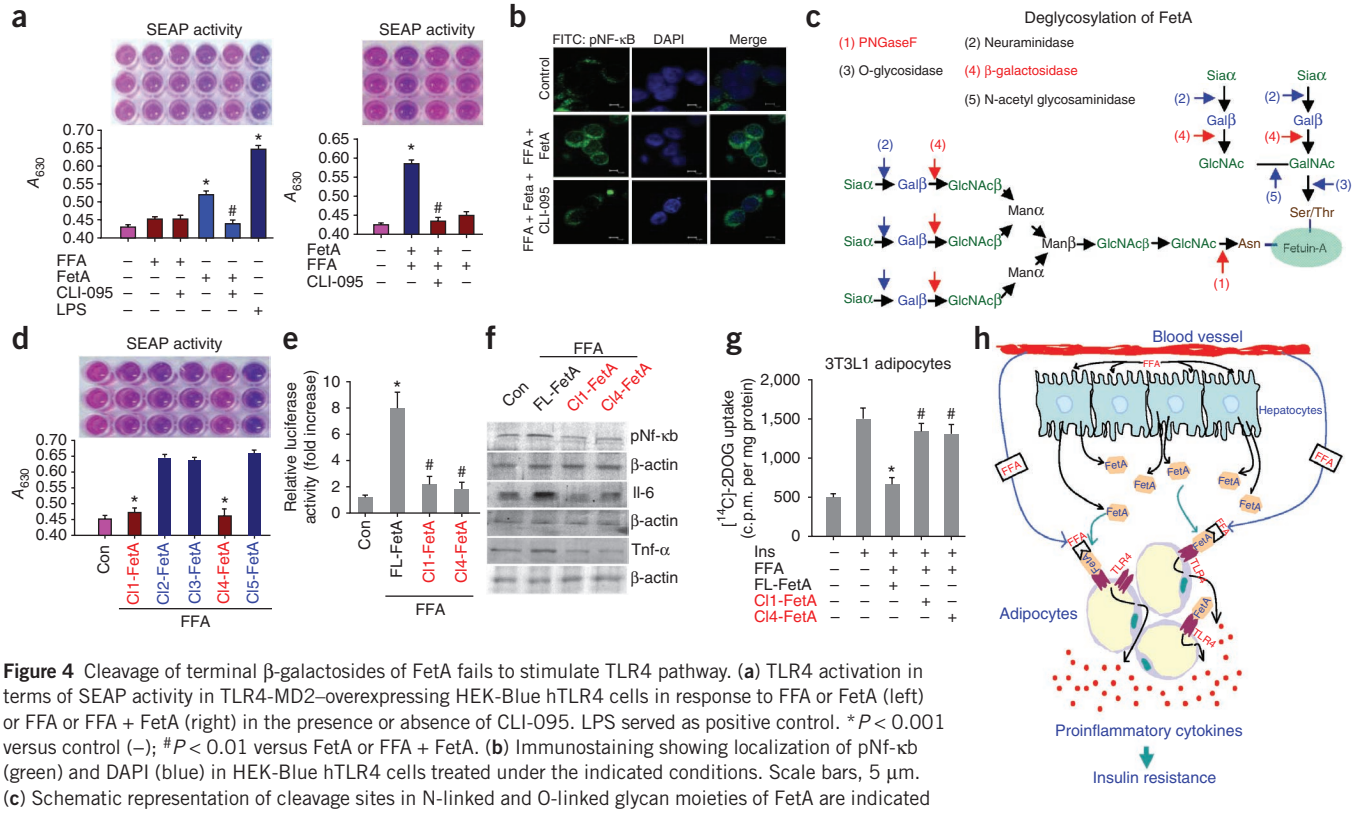

Figure 4 Cleavage of terminal β-galactosides of FetA fails to stimulate TLR4 pathway. (**a**) TLR4 activation in terms of SEAP activity in TLR4-MD2–overexpressing HEK-Blue hTLR4 cells in response to FFA or FetA (left) or FFA or FFA + FetA (right) in the presence or absence of CLI-095. LPS served as positive control. $^{*}P < 0.001$ versus control (–); $^{\#}P < 0.01$ versus FetA or FFA + FetA. (**b**) Immunostaining showing localization of pNf-κb (green) and DAPI (blue) in HEK-Blue hTLR4 cells treated under the indicated conditions. Scale bars, 5 μm. (**c**) Schematic representation of cleavage sites in N-linked and O-linked glycan moieties of FetA are indicated by red and blue arrows. Sia, sialic acid; Gal, galactose; Man, mannose; GlcNAc, N-acetylglucosamine; GalNAc, N-acetylgalactosamine; Asn, Asparagine, Ser/Thr: Serine/Threonine. (**d**) Inhibition of SEAP activity in response to cleaved FetAs (Cl1 and Cl4) by PNGaseF and β-galactosidase enzymes. $^{*}P < 0.001$ versus Cl2, Cl3 and Cl5. (**e**) Inhibition of Nf-κb reporter activity in 3T3L1 adipocytes treated with FFA plus Cl1 or Cl4 FetA. $^{*}P < 0.001$ versus Control (–); $^{\#}P < 0.01$ versus full-length FetA (FL-FetA). (**f**,**g**) Western blot showing pNf-κb, Il-6 and Tnf-α abundance in 3T3L1 adipocytes (**f**) and [^{14}C]-2DOG uptake by 3T3L1 adipocytes (**g**) incubated with FL or cleaved FetAs (Cl1 and Cl4). $^{*}P < 0.01$ versus Ins; $^{\#}P < 0.01$ versus FL-FetA. Values are means ± s.e.m. (**h**) Proposed model highlighting the requirement of FetA in lipid-induced TLR4 activation that leads to insulin resistance. Error bars represent mean ± s.e.m.

that FFAs have no direct association with TLR4 (refs. 8,9), whereas they bind FetA appreciably[22] (**Supplementary Fig. 3a**). We found further evidence of these facts in a lipid-protein overlay assay where FFAs bound FetA but not TLR4 (**Supplementary Fig. 3b**). Hence, it is possible that FetA acts as an intermediary between FFA and TLR4. Indeed, coimmunoprecipitation revealed the existence of a complex between FetA and TLR4 (**Fig. 3a** and **Supplementary Fig. 3c**).

To study the nature of this complex and to probe the possibility of a physical interaction between FetA and TLR4 as proposed above, we performed surface plasmon resonance (SPR) in which varied concentrations of FetA were flowed over a histidine-tagged human TLR4-myeloid differentiation factor 2 (MD2) complex which was immobilized on a nitrilotriacetic acid (NTA) sensor chip. The resulting sensorgram showed concentration-dependent binding of FetA to TLR4, and the affinity of this binding was appreciably high, as indicated by its K_D value (1.8×10^{-8} M). Reversing the situation, wherein FetA remained immobilized on the carboxymethylated dextran (CM5) chip and TLR4 was used as analyte, produced a similar binding affinity ($K_D = 2.3 \times 10^{-8}$ M) (**Fig. 3b**). The inability of high mobility group A1 (HMGA1) to interact with TLR4 indicates the specificity of this interaction (**Supplementary Fig. 3d**).

To examine whether such a complex between FetA and TLR4 is operative in an intracellular system, we performed a yeast two-hybrid (Y2H) assay using pGBKT7 fused with DNA encoding the extracellular domain or cytosolic domain of Tlr4. These plasmids were separately transfected into the Y2H Gold strain of yeast, followed by mating with the Y187 strain containing full-length *FetA* inserted into pGADT7. FetA interacted with the extracellular domain of Tlr4, as interaction-dependent growth of colonies was observed in SD/–Ade/–His/–Leu/–Trp (quadruple dropout, QDO) plates, whereas colony growth did not occur after mating with yeast expressing the plasmid encoding the cytoplasmic domain of Tlr4 (**Fig. 3c**).

We then searched the probable sites of the TLR4 extracellular domain to which FetA binds. We presumed it could be the region of leucine-rich repeats (LRR), as those have been previously found to be involved in protein-protein interactions[30]. To analyze FetA recognition of specific LRR sites, we mutated different LRRs in *Tlr4*. Deletion mutation of LRR2 (Leu100–Gly123) or LRR6 (Thr493–Thr516) in the extracellular domain of Tlr4 impeded its interaction with FFA+FetA, as indicated by diminished Nf-κb luciferase activity (**Fig. 3d**) and cytokine expression (**Fig. 3e**) in differentiated adipocytes and by α-galactosidase activity in Y2H studies (**Supplementary Fig. 3e**). Deletion mutations at these sites not only restored but also augmented insulin sensitivity (**Fig. 3f**), possibly because of the dominant-negative nature of the mutations (**Fig. 3d**). Mutational studies suggest that these two LRRs of Tlr4 are the crucial sites where FetA binds and permits FFAs to exert their deleterious effect on insulin activity. Hence, it is possible that FFAs, FetA and TLR4 all form one complex. To examine this, we incubated [^{3}H]-palmitate with FetA followed by human TLR4 incubation. Both Coomassie staining and flurography of the native-PAGE gel revealed a ternary complex between the three of them (**Fig. 3g**).

To determine the biological relevance of FetA-TLR4 interactions in FFA-induced insulin resistance, we used genetically engineered HEK-Blue hTLR4 cells, which contain a TLR4–NF-κB–secreted embryonic alkaline phosphatase (SEAP) reporter system to detect TLR4–NF-κB activation. Incubation of FFAs in the presence of FetA enhanced SEAP activity, which was inhibited by CLI-095 (**Fig. 4a**), and this was dose and time dependent (**Supplementary Fig. 4a–c**), indicating that FFA+FetA operates through the TLR4 pathway. Immunofluorescence study further supported the notion that both FetA and TLR4 are required to transduce FFA signals, because FFA+FetA-stimulated nuclear translocation of NF-κB was abrogated by CLI-095 (**Fig. 4b**).

We identified the sequence of TLR4 where FetA binds; however, which part of FetA recognizes the TLR4 sequence remained unanswered. As terminal carbohydrate moieties of glycoproteins, such as sialic acid, galactose and fucose, underpin cell adhesion, receptor recognition and host-pathogen interactions[31], we presumed that the glycan moieties of FetA bind TLR4, especially as Gram-negative bacteria trigger TLR4 signaling through the glycan residues of lipopolysaccharide[32–34]. To investigate this possibility, we used various enzymes to cleave specific glycosidic and amide bonds in FetA, as indicated (**Fig. 4c**). Truncated FetA and FetA's glycan part, obtained by enzymatic cleavage, were separately added to HEK-Blue hTLR4 cells. β-galactosidase– or PNGaseF-cleaved FetA was unable to stimulate SEAP activity (**Fig. 4d** and **Supplementary Fig. 4d**). Given that these results coincided with lower *Nf-κb* promoter activity and a concomitant reduction of proinflammatory cytokines expression (**Fig. 4e**,**f** and **Supplementary Fig. 4e**), the terminal β-galactoside moiety of FetA seems crucial for recognizing TLR4. We show that β-galactosidase–cleaved FetA did not produce FFA-induced insulin resistance in adipocytes (**Fig. 4g**).

The pathway in which FFA–FetA–induced TLR4 activation causes insulin resistance is presented in a schematic diagram (**Fig. 4h**). The influence of dietary lipids on the activation of the TLR4–NF-κB pathway to produce proinflammatory cytokines, resulting in insulin resistance, has long been known. The amount of fat in HFD could be a factor in TLR4-mediated insulin resistance; 45% fat in HFD has been shown to be insufficient to produce such response[35], whereas 55–60% fat in HFD effected insulin resistance through TLR4 (refs. 4,20,36). We have used HFD with 65% fat, which clearly induced insulin resistance. However, the molecular pathways that underlie a FFA-TLR4 interaction continue to elude investigators. FetA is a major carrier protein of FFAs in the circulation[22], and in the absence of FFAs directly binding to TLR4[8,9], we envisioned an endogenous presenter of FFAs to TLR4. We have shown here that FetA serves this purpose, as it physically interacts with both FFAs and TLR4. Moreover, our work has indicated a key role of FetA in FFA-induced TLR4 activation in adipocytes and thus in insulin resistance. These findings further suggest that FetA represents a potentially new target for developing therapeutics in the management of lipid-induced insulin resistance and type 2 diabetes.

METHODS

Methods and any associated references are available in the online version of the paper.

Note: Supplementary information is available in the online version of the paper.

ACKNOWLEDGMENTS

This research was financially supported by a grant from the CSIR and Department of Science and Technology, Ministry of Science and Technology, New Delhi. We thank the National Centre for Cell Science, Pune, India, for providing the 3T3L1 cell line; A. Bandyopadhyay and S. Roy of the Indian Institute of Chemical Biology, Kolkata for their help in the confocal and SPR work, respectively. D.P. is thankful to CSIR, New Delhi, for the award of Senior Research Fellowship. S.D. thanks the University Grants Commission (UGC), New Delhi, for the award of a UGC-Dr. D.S. Kothari postdoctoral fellowship and CSIR-NEIST for a Quick Hire Fellowship. S.B. thanks the Indian National Science Academy for his Senior Scientist position. G.D. gratefully acknowledges the gift of *Tlr4*$^{-/-}$ mice from R. Medzhitov, Yale School of Medicine. The authors appreciate the use of facilities as extended to us by the head of the Department of Zoology, Visva-Bharati University, Santiniketan; the director of IICB, director of IPGME&R-SSKM Hospital, Kolkata; the director of the National Institute of Immunology, director of ICGEB, New Delhi and the director of NEIST, Jorhat, India.

AUTHOR CONTRIBUTIONS

D.P. and S.D. designed and performed all the experiments, analyzed the data and wrote the manuscript; R.K. generated VMO–based *FetA* and *Tlr4* knockdown mice; G.D. performed lipid infusion study in WT and *FetA*^{KD} mice; S.R. provided nondiabetic and diabetic human blood and fat tissue; S.S.M. provided blood and tissue samples from WT and *db*/*db* mice; S. Maitra, G.D., S. Mukhopadhyay and S.S.M. wrote the manuscript; S.B. designed and supervised this study, analyzed the data and wrote the manuscript.

COMPETING FINANCIAL INTERESTS

The authors declare no competing financial interests.

Published online at http://www.nature.com/doifinder/10.1038/nm.2851.
Reprints and permissions information is available online at http://www.nature.com/reprints/index.html.

1. Lee, J.Y., Sohn, K.H., Rhee, S.H. & Hwang, D. Saturated fatty acids, but not unsaturated fatty acids, induce the expression of cyclooygenase-2 mediated through Toll-like receptor 4. *J. Biol. Chem.* **276**, 16683–16689 (2001).
2. Suganami, T. *et al.* Role of the Toll-like receptor 4/NF-κB pathway in saturated fatty acid–induced inflammatory changes in the interaction between adipocytes and macrophages. *Arterioscler. Thromb. Vasc. Biol.* **27**, 84–91 (2007).
3. Nguyen, M.T.A. *et al.* A subpopulation of microphages infiltrates hypertrophic adipose tissue and is activate by free fatty acids via Toll-like receptors 2 and 4 and JNK-dependent pathways. *J. Biol. Chem.* **282**, 35279–35292 (2007).
4. Shi, H. *et al.* TLR4 links innate immunity and fatty acid-induced insulin resistance. *J. Clin. Invest.* **116**, 3015–3025 (2006).
5. Kim, J.K. Fat uses a TOLL-road to connect inflammation and diabetes. *Cell Metab.* **4**, 417–419 (2006).
6. Fessler, M.B., Rudel, L.L. & Brown, J.M. Toll-like receptor signaling links dietary fatty acids to the metabolic syndrome. *Curr. Opin. Lipidol.* **20**, 379–385 (2009).
7. Kim, F. *et al.* Toll-like receptor-4 mediates vascular inflammation and insulin resistance in diet-induced obesity. *Circ. Res.* **100**, 1589–1596 (2007).
8. Schaeffler, A. *et al.* Fatty acid–induced induction of Toll-like receptor-4/nuclear factor-κB pathway in adipocytes links nutritional signalling with innate immunity. *Immunology* **126**, 233–245 (2009).
9. Erridge, C. & Samani, N.J. Saturated fatty acids do not directly stimulate Toll-like receptor signaling. *Arterioscler. Thromb. Vasc. Biol.* **29**, 1944–1949 (2009).
10. Xu, H. *et al.* Chronic inflammation in fat plays a crucial role in the development of obesity-related insulin resistance. *J. Clin. Invest.* **112**, 1821–1830 (2003).
11. Hotamisligil, G.S., Arner, P., Caro, J.F., Atkinson, R.L. & Spiegelman, B.M. Increased adipose tissue expression of tumor necrosis factor-α in human obesity and insulin resistance. *J. Clin. Invest.* **95**, 2409–2415 (1995).
12. de Luca, C. & Olefsky, J.M. Stressed out about obesity and insulin resistance. *Nat. Med.* **12**, 41–42 (2006).
13. Qatanani, M. & Lazar, M.A. Mechanisms of obesity-associated insulin resistance: many choices on the menu. *Genes Dev.* **21**, 1443–1455 (2007).
14. Mori, K. *et al.* Association of serum fetuin-A with insulin resistance in type 2 diabetic and nondiabetic subjects. *Diabetes Care* **29**, 468 (2006).
15. Stefan, N. *et al.* Plasma fetuin-A levels and the risk of type 2 diabetes. *Diabetes* **57**, 2762–2767 (2008).
16. Ix, J.H. & Sharma, K. Mechanisms linking obesity, chronic kidney disease, and fatty liver disease: the roles of fetuin-A, adiponectin, and AMPK. *J. Am. Soc. Nephrol.* **21**, 406–412 (2010).
17. Dasgupta, S. *et al.* NF-κB mediates lipid-induced fetuin-A expression in hepatocytes that impairs adipocyte function effecting insulin resistance. *Biochem. J.* **429**, 451–462 (2010).
18. Hennige, A.M. *et al.* Fetuin-A induces cytokine expression and suppresses adiponectin production. *PLoS ONE* **3**, e1765 (2008).
19. Mathews, S.T. *et al.* Improved insulin sensitivity and resistance to weight gain in mice null for the *Ahsg* gene. *Diabetes* **51**, 2450–2458 (2002).
20. Tsukumo, D.M.L. *et al.* Loss-of-function mutation in TLR4 prevents diet-induced obesity and insulin resistance. *Diabetes* **56**, 1986–1998 (2007).
21. Mathews, S.T. *et al.* Fetuin null mice are protected against obesity and insulin resistance associated with aging. *Biochem. Biophys. Res. Commun.* **350**, 437–443 (2006).

22. Cayatte, A.J., Kumbla, L. & Ravi Subbiah, M.T. Marked acceleration of exogenous fatty acid incorporation into cellular triglycerides by fetuin. *J. Biol. Chem.* **265**, 5883–5888 (1990).
23. Jiao, P. *et al.* Obesity-related upregulation of monocyte chemotactic factors in adipocytes involvement of nuclear factor-κB and c-Jun NH2–terminal kinase pathways. *Diabetes* **58**, 104–115 (2009).
24. Zu, L. *et al.* Bacterial endotoxin stimulates adipose lipolysis via Toll-like receptor 4 and extracellular signal-regulated kinase pathway. *J. Biol. Chem.* **284**, 5915–5926 (2009).
25. Mellgren, R.L. & Huang, X. Fetuin A stabilizes m-calpain and facilitates plasma membrane repair. *J. Biol. Chem.* **282**, 35868–35877 (2007).
26. Davis, J.E., Gabler, N.K., Daniel, J.W. & Spurlock, M.E. Tlr-4 deficiency selectively protects against obesity induced by diets high in saturated fat. *Obesity (Silver Spring)* **16**, 1248–1255 (2008).
27. Schwartz, E.A. *et al.* Nutrient modification of the innate immune response: a novel mechanism by which saturated fatty acids greatly amplify monocyte inflammation. *Arterioscler. Thromb. Vasc. Biol.* **30**, 802–808 (2010).
28. Barton, G.M. & Medzhitov, R. Toll-like receptor signaling pathways. *Science* **300**, 1524–1525 (2003).
29. Kawai, T. & Akira, S. TLR signaling. *Cell Death Differ.* **13**, 816–825 (2006).
30. Medzhitov, R., Preston-Hurlburt, P. & Janeway, C.A.J. A human homologue of the *Drosophila* Toll protein signals activation of adaptive immunity. *Nature* **388**, 394–397 (1997).
31. Paulson, J.C. & Colley, J.C.J. Glycosyltransferases. Structure, localization, and control of cell type-specific glycosylation. *J. Biol. Chem.* **264**, 17615–17618 (1989).
32. Park, B.S. *et al.* The structural basis of lipopolysaccharide recognition by the TLR4–MD-2 complex. *Nature* **458**, 1191–1195 (2009).
33. Barata, T.S., Teo, I., Brocchini, S., Zloh, M. & Shaunak, S. Partially glycosylated dendrimers block MD-2 and prevent TLR4–MD-2–LPS complex mediated cytokine responses. *PLoS Comput. Biol.* **7**, e1002095 (2011).
34. Ohto, U., Fukase, K., Miyake, K. & Satow, Y. Crystal structures of human MD-2 and its complex with antiendotoxic lipid IVa. *Science* **316**, 1632–1634 (2007).
35. Orr, J.S. *et al.* Toll-like receptor 4 deficiency promotes the alternative activation of adipose tissue macrophages. *Diabetes* published online, doi:10.2337/db11-1595 (29 June 2012).
36. Suganami, T. *et al.* Attenuation of obesity-induced adipose tissue inflammation in C3H/HeJ mice carrying a Toll-like receptor 4 mutation. *Biochem. Biophys. Res. Commun.* **354**, 45–49 (2017).

ONLINE METHODS

Animals and treatments. In the present study, we used control (C57BLKS/6J) and *db/db* (BKS.Cgm+/+Lepr(db)/J, stock no. 000642) female mice obtained from the Jackson Laboratory, using five mice in each treatment group. We made mice insulin resistant by providing HFD for 12 weeks. In percentage of total energy, the HFD consisted of 32.5% lard, 32.5% corn oil, 20% sucrose and 15% protein, whereas the SD contained 57.3% carbohydrate, 18.1% protein and 4.5% fat. The energy content of the standard diet was 15 kJ/g and the high-fat diet was 26 kJ g^{-1}. We procured Fetuin-A (5′-AAGACCAGG GACTTCATGGTTGCTC-3′; accession code: NM_013465.1), TLR4 (5′-AT GCAAGAGAGGCATCATCCTGGCA-3′; accession code: NM_019178.1) and their control VMOs from Gene Tools to generate $FetA^{KD}$ and $TLR4^{KD}$ mice. We treated 5- to 6-week-old female BALB/c mice with these VMOs. Twenty-five nmoles of VMO was delivered to tail vein through injection in each mouse for 5 consecutive days, one on each day. We also used $Tlr4^{-/-}$ mice, which were backcrossed ten generations on C57BL/6 background. WT littermates were used as controls. We determined GTT by estimating blood glucose concentration before and after oral gavages of 1g glucose per kg body weight at the indicated time points using Accu-Chek glucometer (Roche). ITT was assessed in a similar way by injecting 0.7 U insulin per kg body weight. We infused (1 µl h^{-1}) palmitate (600 mM) or saline for 8 d via a subcutaneous miniosmotic pump (Alzet, DURECT Corporation; Model 2001). Plasma insulin level was estimated by using Accu-Bind insulin ELISA kit (Monobind). Insulin function was evaluated by HOMA-IR and calculated as fasting insulin (µU per liter) × fasting glucose (mg dl^{-1})/405 (ref. 37). Mouse FetA (0.7 mg per g body weight) was administered in SD- and HFD-fed $FetA^{KD}$ mice by intravenous injection. Control mice received equal volumes of sterile PBS. All mouse experiments were performed following the guidelines prescribed by and with the approval of the Animal Ethics Committees of Visva-Bharati, International Centre of Genetic Engineering and Biotechnology and National Institute of Immunology.

Fetuin-A purification and deglycosylation. We purified FetA following the procedure of Li *et al.*[38] with slight modifications. We collected human and mouse serum and filtered through Amicon ultra-100K and 50K membrane filter devices (UFC510096 and UFC505096, Amicon Ultra Centrifugal Filters, Millipore) to obtain proteins between 50 kDa and 100 kDa. Samples were subjected to gel filtration chromatography using a HiPrep 26/60 Sephacryl S-100 high-resolution column. We loaded the FetA-enriched fraction on a column to remove serum albumin/IgGs (Pierce albumin/IgG removal kit, 89875). FetA-enriched elutant was then loaded onto a 5-ml Hitrap SP HP column, and bound FetA was collected by a linear NaCl gradient (50 mM sodium acetate). Purity of FetA was checked by SDS-PAGE (**Supplementary Fig. 1f**). We purchased a protein deglycosylation kit (Sigma, cat. no. EDEGLY) and used it for selective removal of glycan from FetA by PNGase F, α(2 3,6,8,9)-neuraminidase, O-glycosidase, β(1 4)-galactosidase and β-N-acetylglucosaminidase enzymes.

Removal of endotoxin contamination. We used EndoClear kit (EndoClear kit HIT307; Hycult Biotech) to remove endotoxin content in FFA (palmitate) and FetA preparations according to the manufacturer's instructions. Mouse FetA contained about 0.06 endotoxin units (EU) per ml and human FetA had around 0.08 EU ml^{-1} endotoxin. The endotoxin level of BSA-palmitate conjugate was 2.2 EU ml^{-1}. We passed all of the preparations separately through an EndoTrap Blue column to remove endotoxin contamination. Eluent was subsequently examined by Chromogenic Limulus Amebocyte Lysate (LAL) assay kit (HIT311, Hycult Biotech) to detect its endotoxin level. We repeated this removal procedure for several times until to the endotoxin concentration was very negligible, that is, 0.005–0.009 EU ml^{-1} (**Supplementary Fig. 1e**). We checked these levels of endotoxin by administering the preparations to 3T3L1 adipocytes and macrophages, which failed to produce a TLR4 response.

To further examine whether this negligible level of LPS could influence FetA- or FFA–FetA induced TLR4 activation, we conducted two experiments. First, Polymixin B (PMB) was incubated with adipocytes and macrophages in the presence of LPS, FFA, FetA or FFA+FetA followed by determination of TLR4 activity through NF-κB promoter reporter assay. PMB did not interfere with FetA- or FFA+FetA–induced TLR4 activation but blocked LPS-induced activation of TLR4 (**Supplementary Fig. 1f**). Second, we checked whether LPS binds FetA by incubating 60 EU per ml LPS (normal level of LPS in human serum[39]) with FetA and subjecting it to coimmunoprecipitation followed by western blotting with *Escherichia coli* LPS–specific mouse monoclonal antibody (clone number: 2D7/1; cat. no. ab35654, Abcam; dilution: 1:500 to show that LPS interacted with FetA (**Supplementary Fig. 1g**), which was also evident from TLR4 activation (**Supplementary Fig. 1h**).

Cell cultures and treatments. We isolated primary hepatocytes and peritoneal macrophages from WT and $Tlr4^{KD}$ mice and primary adipocytes and peritoneal macrophages from WT and $TLR4^{-/-}$ mice and incubated them with FetA for 4 h in DMEM/F12. 3T3L1 preadipocyte and RAW264.7 macrophage cells were cultured in DMEM containing penicillin (100 U ml^{-1}) and streptomycin (100 µg ml^{-1}) and supplemented with 10% FBS at 37 °C in humidified atmosphere with 5% CO_2. Two days after confluence, preadipocytes were stimulated to differentiate over 5 d in differentiation medium supplemented with 5 µg ml^{-1} insulin, 0.5 mmol per liter 3-isobutyl-1-methylxanthine and 1 µmol per liter dexamethasone. As conventionally used culture media usually contain 10% FBS that has substantial amount (~2 mg ml^{-1}) of FetA[25]. we washed differentiated 3T3L1 adipocytes thoroughly to remove FetA contamination, if any, and then carried out incubations/treatments with serum-free medium (SFM) without antibiotics. HEK-Blue hTLR4 cells (cat. no. hkb-htlr4) containing TLR4/NF-κB/SEAP [TLR4-NF-κB-SEAP] reporter was purchased from Invivogen, CA, USA, and was incubated at various concentrations (25, 50, 100 and 200 µg ml^{-1}) of FetA in the presence of 0.75 mM palmitate or different concentrations of palmitate (0.25, 0.50, 0.75 and 1.0 mM) with a fixed concentration of FetA (100 µg ml^{-1}). We performed time kinetics with 15, 30, 60, 120 and 240 min of incubation where both FetA (100 µg ml^{-1}) and palmitate (0.75 mM) were used at a fixed concentration. In case of cell incubations with inhibitors, CLI-095 (3 µM) or U0126 (10 µM) or polymixin B (100 µg ml^{-1}) were added 1 h before addition of FFA or FetA or both. In positive-control treatments, LPS (100 ng ml^{-1}) was used as TLR4 agonist for 4 h. We transfected MyD88 or TLR4 siRNA or wild-type TLR4 or mutated TLR4 vector into 3T3L1 adipocytes with Lipofectamine 2000 (Invitrogen, Carlsbad, CA, USA) following the manufacturer's protocol. Upon termination of incubations, cells were washed twice with ice-cold PBS and harvested with trypsin (0.25%)–EDTA (0.5 mM). NF-κB promoter reporter activity was assessed according to the manufacturer's instructions using Steady-Glo luciferase assay system (PromegaA) in cells transfected with pNF-κB-luc expression vector (PathDetect NF-κB *cis*-reporting system, Stratagene).

Human subjects. We obtained visceral adipose tissue from ten individuals with diabetes (four males and six females) and 12 individuals without diabetes (six males and six females), 54–69 years old, who were admitted to IPGME&R-SSKM Hospital and underwent abdominal surgery. With the due ethical committee clearance from the hospital, the Institutional Ethics Committee (IEC) approved the study and all the participants in this study gave written consent we also obtained blood and adipose tissue sample from the patients for the estimation of serum FetA level and inflammatory cytokines expression, respectively. Adipose tissue was rinsed with sterile 0.9% NaCl solution followed by washing with HBSS supplemented with 5.5 mM glucose. Adipose tissue was digested in HBSS buffer containing 5.5 mM glucose, 5% fatty acid-free BSA and 3.3 mg ml^{-1} type II collagenase for 30 min in a 37 °C water bath. The digestion mixture was passed through a tissue sieve and adipocytes were resuspended in SFM. Cells were plated in six-well culture plates and kept in a humidified 95% O_2/5% CO_2 atmosphere at 37 °C.

Reagents and antibodies. All tissue culture materials were obtained from Gibco-BRL/Life Technologies, Gaithersburg, USA. 3T3L1 preadipocyte cell differentiation was done by using Adipogenesis assay kit (cat. no. 10006908, Cayman Chemical Company). [U-^{14}C]-2- deoxyglucose (2-DOG) (cat. no. NEC042V250UC; specific activity 250–360 mCi per mmol) and [9,10-^{3}H(N)]-palmitate (cat. no. NET043005MC; specific activity 30–60 C per mmol) were obtained from GE Healthcare, and 5-ml Hitrap SP HP columns (cat. no. 17-1152-01), HiPrep 26/60 Sephacryl S-100 high resolution

doi:10.1038/nm.2851

columns (cat. no. 17-1165-01), HMW Native molecular weight marker (cat. no. 17-0445-01) and Amersham Hybond-C Extra (cat. no. RPN2020E) were obtained from GE Healthcare. [γ-^{32}P]ATP (cat. no. LCP 101; specific activity, 3800 Ci per mmol) was procured from Board of Radiation and Isotope Technology (BRIT). We purchased antibodies raised against pNF-κB p65 (Ser536 (cat. no. sc-101752)), IL-6 (sc-81026 and sc-1265), TNF-α (sc-1350), TLR4 (sc-10741) and FetA (sc-28924) from Santa Cruz Biotechnology. Anti-IκBα antibody (cat. no. 9242) was procured from Cell Signaling Technology and anti–*Escherichia coli* LPS antibody (cat. no. ab35654) was purchased from Abcam, Cambridge, MA, USA. Alkaline phosphatase–conjugated goat anti-rabbit antibodies, rabbit anti-goat antibodies, polymixin B sulfate and U0126 ethanolate were purchased from Sigma Chemical Co, Bethesda, MA, USA. PageRuler Prestained Protein Ladder (cat. no. SM0671) was obtained from Fermentas, Maryland, USA. Recombinant human TLR4 protein (cat. no. 3146/CF), human and mouse FetA DuoSet ELISA kit (cat. nos. DY1184 and DY1563), IL-6 and TNF-α Quantikine ELISA kit (cat. no. M6000B and cat. no. MTA00B) were purchased from R&D Systems, Minneapolis, MN, USA. All the primary antibodies used in western blotting at a dilution of 1:500 and secondary antibodies were used at 1:2,000 dilution. We have obtained purified human Fetuin-A and recombinant mouse FetA from Prospec Tany TechnoGene Ltd., East Brunswick, MN, USA (cat. no. PRO-418) and R&D Systems, Inc., Minneapolis, MN, USA (cat. no. 1563-PI-050), respectively. CLI-095 (cat. no. tlrl-cli95) and Ultrapure-Lipopolysaccharide (LPS) from *E. coli* 0111: B4 (cat. no. tlrl-pelps) were purchased from Invivogen, CA, USA. Human RT^2 Prolifer PCR array and all other RT^2-qPCR primers: *TLR4* (cat. no. PPH01795E (68 bp); *Tlr4* (cat. no. PPM04207F (93 bp); *FETA* (cat. no. PPH16956E (142 bp); *FetA* (cat. no. PPM32919B (170 bp), *IL6* (cat. no. PPH00560B (160 bp); *Il6* (cat. no. PM03015A (178 bp); *TNFα* (cat. no. PPH00341E (54 bp); *Tnfα* (cat. no. PM03113F (93 bp); *GAPDH* (cat. no. PPH00150E (175 bp); *Gapdh* (cat. no. PPM02946E (140 bp) were purchased from SA Biosciences, Frederick, MD, USA. We procured the Matchmaker Gold yeast two-hybrid system (cat. no. 630489) and QuickChange site-directed mutagenesis kit (cat. no. 200518) from Clontech Laboratories and Stratagene, respectively. Pierce albumin/IgG removal kit (cat. no. 89875) was obtained from Pierce. All other chemicals were procured from Sigma-Aldrich.

Western blots. We determined protein concentration of tissue extract or cell lysates or media following a previously described method[40]. We resolved 50 μg of protein sample on 10% SDS-PAGE and transferred it to PVDF membranes (Millipore) with the help of Semi-Dry Trans-Blot SD Cell (Bio-Rad Laboratories). The membranes were first incubated with primary antibody at 1:500 dilutions followed by goat anti-rabbit secondary antibody conjugated with alkaline phosphatase at 1:2,000 dilutions using SNAP ID apparatus (Millipore). The protein bands were detected by using 5-bromro 4-chloro 3-indolyl phosphate/nitroblue tetrazolium (BCIP/NBT).

Quantitative PCR. We extracted RNA from tissues or cells by using RNeasy Lipid Tissue Mini Kit (Qiagen) according to the manufacturer's instructions. RNA was treated with DNase I and reverse transcribed using Revert Aid first-strand cDNA synthesis kit (Fermentas). We used SYBR green–based real-time quantitative PCR reactions (Applied Biosystems) by using gene-specific primers obtained from SA Biosciences, Frederick, MD, USA. After the final extension, a melting curve analysis was performed to ensure the specificity of the products. *Gapdh* was simultaneously amplified in separate reactions and used for correcting the C_t value.

PCR array. We performed human Toll-like receptor signaling pathway PCR array (cat. no. PAHS-018A, SA Bioscience) by following the manufacturer's instructions. Briefly, first-strand cDNA was synthesized from 5 μg of RNA using the RT^2 First Strand Kit. A total volume of 25 μl of PCR reaction mixture, which included 12.5 μl of RT^2 Real-Time SYBR Green/ROX PCR master mix, 11.5 μl of nuclease-free water and 1 μl of template cDNA, was loaded in each well of the RT^2 Profiler PCR array. PCR amplification was performed in an ABI 7500 real-time PCR machine (Applied Biosystems). Data were imported into RT2 Proflier PCR array data analysis, version 3.5 to detect the alterations of gene expression. C_t values were normalized to housekeeping genes.

Eelectrophoretic mobility shift assay. We prepared nuclear extracts from cells under different incubations and subjected to electrophoretic mobility shift assay using oligonucleotide probes specific for the NF-κB binding site (5′-GCACCTGGGTTGGTCCCGAAGC-3′) as described previously[41]. The probes were end-labeled with $^{\gamma 32}$P-[ATP] using T4 polynucleotide kinase and incubated with 10 μg of nuclear extracts in a 20-μl reaction volume for 45 min on ice. Reaction mixture was resolved on a 5% (wt/vol) non-denaturing polyacrylamide gel and exposed to the phosphorimager screen, and the DNA/protein complexes were revealed on Storm phosphor-imager (GE Healthcare).

Chromatin immunoprecipitation assay. We performed ChIP by using ChIP assay kit (Upstate) according to our previous description[41] using 2 μg of anti–NF-κBp65 or anti-IgG antibodies. Primers used for amplification of the human *IL6* promoter sequence were 5′-CAGAGCACCTGGTTGGT-3′ (forward) and 5′-GCCCCAGAGCTGAGCAA-3′ (reverse). PCR products were run on ethidium bromide–stained 1.5% agarose gel, and the image was captured by the Bio-Rad gel documentation system using Image Lab software.

Coimmunoprecipitation. We conducted our coimmunoprecipitation study by following a method previously described[41]. Briefly, 200 μg of pure human FetA and Tlr4 proteins were incubated for 4 h followed by overnight incubation with FetA- or TLR4-specific antibody. The immunocomplex was precipitated with a 4-h incubation of protein-A agarose. Pelleted immunocomplex was washed thoroughly, boiled in 4× sample buffer, vortexed and then centrifuged at 15,000 r.p.m. for 10 min. Supernatant was isolated and run on 10% SDS-PAGE gel. This was followed by immunoblotting with either antibodies specific to TLR4 or FetA. Similarly, 200 μg of LPS was incubated with either FetA or TLR4 and subjected to immunoprecipitation by FetA- or TLR4-specific antibody followed by immunoblotting with LPS-specific antibody.

Lipid-protein overlay assay. We performed protein-lipid overlay assay by following an earlier description[42] with little modification. Briefly, the nitrocellulose membrane was spotted with increasing amounts of palmitate (1, 3 and 5 mM), and the membrane was blocked for 1 h in 2 ml of blocking buffer (3% fatty-acid-free BSA, 150 mM NaCl, 10 mM Tris pH 7.4) followed by incubation with 200 ng ml^{-1} of purified FetA or TLR4 protein overnight at 4 °C. The membrane was then incubated with a 1:500 dilution of anti-FetA or anti-TLR4 antibody for 1 h followed by 1 h incubation with 1:2,000 dilution of ALP-conjugated goat anti-rabbit secondary antibody, and FFA-bound protein was visualized by BCIP-NBT.

Immunofluorescence. We incubated paraformaldehyde-fixed cells overnight with anti–pNF-κBp65 polyclonal antibodies (dilution 1:100) followed by FITC-conjugated goat anti-rabbit secondary antibody (dilution 1:1,000) for 2 h. Cells were mounted in anti-fade mounting medium containing DAPI (Vector Laboratories, Inc.) for nuclear staining and followed by analysis with a laser scanning confocal microscope (Leica 224).

Surface plasmon resonance (BIAcore) study. We performed surface plasmon resonance experiments on a BIAcore 3000 instrument (BIAcore) using NTA and CM5 sensor chips according to manufacturer's instructions. Briefly, the NTA sensor chip was equilibrated with running buffer containing 10 mM HEPES (pH 7.5), 150 mM NaCl, 0.005% Surfactant P20, 50 mM EDTA) followed by priming the chip with 0.1 M $NiCl_2$. Pure His(C-terminal)-TLR4/MD2 complex was flowed over the Ni^{2+}-coated NTA sensor chip surface at a flow rate of 5 μl min^{-1}. The final amount of His-TLR4 protein covalently immobilized on the surface was 600 RU. Varied concentrations of FetA (25–100 nM) was sprayed over the immobilized TLR4 Ni^{2+}-primed NTA chip at a flow rate of 5 μl min^{-1} for 10 min. The CM5 sensor chip was used to direct immobilization of FetA by the amine-coupling method and followed by TLR4 protein run at various concentrations (10–100 nM) over it. In both cases, the sensorgram was corrected by subtracting the initial level of SPR signal before injection of the FetA or TLR4 and plotted as RU versus time. Binding kinetics were analyzed for one-to-one Langmuir binding model provided with BIA evaluation software. provided with BIA evaluation software.

Yeast two-hybrid assay. We conducted two-hybrid assays following the manufacturer's protocol of Matchmaker-Gold yeast two-hybrid assay kit. For this purpose we first amplified the extracellular domain or cytoplasmic domain of TLR4 and full-length FetA by PCR from adipocyte and hepatocyte cDNAs, respectively, followed by their cloning into pGBKT7 or pGADT7 vector flanked by EcoRI-BamHI. Constructs were in frame and sequenced to confirm the inserts. Primers used for this study are listed in **Supplementary Table 1**. Y2H-Gold strain bearing pGBKT7-ECD or CD of TLR4 vector were mated with Y187 strain bearing FetA-inserted pGADT7 vector. Yeast transformed with plasmids pGBKT7-P53 plus pGADT7-T or pGBKT7-lam plus pGADT7-T served as positive and negative controls, respectively. Growth was assessed on SD/−Ade/−His/−Leu/−Trp (quadruple dropout, QDO) plates incubated at 30 °C for 3 d.

Site-directed mutagenesis. A pCMV6-TLR4 construct containing 3.2 kb of mouse *Tlr4* gene (NM_021297) was purchased from OriGene Technologies. We used this vector as template for the generation of mutant plasmids with the help of the QuikChange site-directed mutagenesis system (Stratagene). We used SMART (simple modular architecture research tool; http://smart.embl.de/) and TollML (database of Toll-like receptor structural motifs; http://tollml.lrz.de/) web-based tools for the identification of leucine-rich repeats (LRRs) on TLR4. Forward and reverse primer sequences used for mutated TLR4 plasmid construction are listed in **Supplementary Table 2**.

[^{14}C] 2-DOG uptake. We incubated skeletal muscle cells or adipocytes with FFA in the absence or presence of FetA for 4 h followed by insulin (100 nM) stimulation for 30 min. [^{14}C] 2-DOG (0.4 nmol ml^{-1}) was added to each incubation 5 min before the termination of experiment. Cells were washed three times with ice-cold KRB buffer in the presence of 0.3 mM phloretin and then solubilized with 1% NP-40. [^{14}C]-2-DOG uptake was measured in a liquid scintillation counter (PerkinElmer Tri-Carb 2800TR).

Statistical analyses. We statistical analyzed the data by using a Student's unpaired *t* test or one-way analysis of variance, where the *F* value indicated significance; means were compared by *post hoc* multiple-range test. All values are mean ± s.e.m. *P* values < 0.05 was considered statistically significant.

37. Matthews, D.R. *et al.* Homeostasis model assessment: insulin resistance and beta-cell function from fasting plasma glucose and insulin concentrations in man. *Diabetologia* **28**, 412–419 (1985).
38. Li, W. *et al.* A hepatic protein, fetuin-a, occupies a protective role in lethal systemic inflammation. *PLoS ONE* **6**, e16945 (2011).
39. Lassenius, M.I. *et al.* Bacterial endotoxin activity in human serum is associated with dyslipidemia, insulin resistance, obesity, and chronic inflammation. *Diabetes Care* **34**, 1809–1815 (2011).
40. Lowry, O.H., Rosebrough, N.J., Farr, A.E. & Randall, R.J. Protein measurement with Folin phenol reagent. *J. Biol. Chem.* **193**, 265–275 (1951).
41. Dasgupta, S. *et al.* Mechanism of lipid induced insulin resistance: Activated PKCε is a key regulator. *Biochim. Biophys. Acta* **1812**, 495–506 (2011).
42. Dowler, S. *et al.* Protein lipid overlay assay. *Sci. STKE* **2002**, pl6 (2002).

doi:10.1038/nm.2851

BJ www.biochemj.org

Biochem. J. (2010) **429**, 451–462 (Printed in Great Britain) doi:10.1042/BJ20100330

online data

NF-κB mediates lipid-induced fetuin-A expression in hepatocytes that impairs adipocyte function effecting insulin resistance

Suman DASGUPTA*[1], Sushmita BHATTACHARYA*[1], Anindita BISWAS*, Subeer S. MAJUMDAR†, Satinath MUKHOPADHYAY‡, Sukanta RAY‡ and Samir BHATTACHARYA*[2]

*Cellular and Molecular Endocrinology Laboratory, Department of Zoology, School of Life Science, Visva-Bharati (A Central University), Santiniketan 731235, India, †Division of Cellular Endocrinology, National Institute of Immunology, Aruna Asaf Ali Marg, New Delhi 110067, India, and ‡Department of Endocrinology and Metabolism, I.P.G.M. E&R/S.S.K.M. Hospital, Kolkata 700020, India

Fetuin-A, a hepatic secretory protein, has recently been implicated in insulin resistance and Type 2 diabetes. It is an endogenous inhibitor of insulin receptor tyrosine kinase. However, regulation of fetuin-A synthesis in relation to insulin resistance is unclear. In the present paper, we report that both non-esterified ('free') fatty acids and fetuin-A coexist at high levels in the serum of *db*/*db* mice, indicating an association between them. For an in-depth study, we incubated palmitate with HepG2 cells and rat primary hepatocytes, and found enhanced fetuin-A secretion to more than 4-fold over the control. Interestingly, cell lysates from these incubations showed overexpression and activity of NF-κB (nuclear factor κB). In NF-κB-knockout HepG2 cells, palmitate failed to increase fetuin-A secretion, whereas forced expression of NF-κB released fetuin-A massively in the absence of palmitate. Moreover, palmitate stimulated NF-κB binding to the fetuin-A promoter resulting in increased reporter activity. These results suggest NF-κB to be the mediator of the palmitate effect. Palmitate-induced robust expression of fetuin-A indicates the occurrence of additional targets, and we found that fetuin-A severely impaired adipocyte function leading to insulin resistance. Our results reveal a new dimension of lipid-induced insulin resistance and open another contemporary target for therapeutic intervention in Type 2 diabetes.

Key words: adipogenesis, fetuin-A, insulin resistance, non-esterified ('free') fatty acid, nuclear factor κB (NF-κB), Type 2 diabetes.

INTRODUCTION

Fetuin-A [α_2 Heremans–Schmid glycoprotein (*AHSG*)] is synthesized primarily in human liver and secreted into serum. In human beings, it is associated with insulin resistance and Type 2 diabetes [1–3]. Fetuin-A is an endogenous inhibitor of insulin receptor tyrosine kinase phosphorylation and abrogates insulin-stimulated downstream signals [4–6]. This inhibitory activity of fetuin-A has been evaluated in a number of *in vitro* and *in vivo* studies across different species levels, including human beings and was found to be strictly conserved [7,8]. Fetuin-A-knockout mice exhibit improved insulin sensitivity [6,9]. The human fetuin-A gene is located on chromosome 3q27 and has been identified as the Type 2 diabetes susceptibility locus [10]. Although fetuin-A is poised to be a potential factor in affecting insulin resistance and Type 2 diabetes, little is known about the regulation of its synthesis in liver. However, a few reports suggest an involvement of lipid on fetuin-A synthesis. In fatty livers which favour the development of Type 2 diabetes [11], a significant increase in fetuin-A levels [12] and its mRNA expression [13] could be detected, whereas a decrease in liver fat in humans is associated with the decline of plasma fetuin-A [12]. Consistently higher levels of circulatory fetuin-A have been observed in high-fat-fed animals and obese diabetic patients [12,13], whereas fetuin-A-null mice are shown to be protected against obesity and insulin resistance [6]. All of these reports indicate a relationship between lipid and fetuin-A to promote insulin resistance, but direct evidence of its up-regulation by lipid is still lacking.

A few recent reports indicate that, despite fetuin-A's classical inhibitory effect on insulin resistance through the down-regulation of insulin receptor activity, its association with adipogenesis may also be an additional factor that amplifies fetuin-A's attenuating effect on insulin activity, thus aggravating insulin resistance. Human visceral adiposity associated with incident diabetes in older persons is a consequence of higher fetuin-A levels [3]. A polymorphism in the gene encoding human fetuin-A is found to adversely affect insulin action in adipocytes [14]. Fetuin-A has also been shown to repress adiponectin production in animals and humans [15], which will obviously adversely affect adipogenesis. This information indicates fetuin-A's inhibitory effect on adipocyte function, but specific information on this aspect of fetuin-A's effects is still scant.

It should be evident from the above description that fetuin-A is closely associated with insulin resistance and, since this is central to the pathophysiology of Type 2 diabetes, understanding of the regulation of fetuin-A synthesis is extremely important. In the present paper, we report that FA (fatty acid) significantly enhanced fetuin-A expression in the human liver cell line HepG2 by increasing NF-κB (nuclear factor κB) binding to its promoter. In lipid-induced fetuin-A expression, C/EBPβ

Abbreviations used: ADM, adipocyte differentiation medium; aP2, adipocyte protein 2; CD36, cluster of differentiation 36; C/EBPβ, CCAAT/enhancer-binding protein β; ChIP, chromatin immunoprecipitation; DMEM, Dulbecco's modified Eagle's medium; 2-DOG, 2-deoxyglucose; EMSA, electrophoretic mobility-shift assay; FA, fatty acid; FAT, fatty acid translocase; FBS, fetal bovine serum; GAPDH, glyceraldehyde-3-phosphate dehydrogenase; GLUT4, glucose transporter 4; HBSS, Hanks buffered saline solution; HFD, high-fat diet; IL-6, interleukin 6; KRP, Krebs–Ringer phosphate; MEM, minimum essential medium; NEFA, non-esterified ('free') fatty acid; NF-κB, nuclear factor κB; NP-40, Nonidet P40; PDTC, pyrrolidine dithiocarbamate; PPARγ, peroxisome-proliferator-activated receptor γ; RT, reverse transcription; siRNA, short interfering RNA; TNFα, tumour necrosis factor α.

[1] These authors contributed equally to this work.

[2] To whom correspondence should be addressed (email bhattacharyasa@gmail.com).

(CCAAT/enhancer-binding protein β) has no role; however, it was shown to be involved in glucocorticoid-induced fetuin-A expression [16]. In NF-κB-knockout HepG2 cells, FA fails to augment fetuin-A synthesis, whereas its expression is greatly increased in the cells transfected with pCMV-NF-κBp65 vector. Up-regulated fetuin-A expression due to lipid may worsen insulin resistance by impairing adipocyte function.

MATERIALS AND METHODS

Reagents and antibodies

All tissue culture materials were obtained from Gibco-BRL/Life Technologies. FAs were purchased from Sigma. [^{3}H]Leucine (specific activity 1000 Ci/mmol), [^{3}H]2-DOG (2-deoxyglucose) (specific activity 12.0 Ci/mmol), [γ-^{32}P]ATP (specific activity 6000 Ci/mmol) and [^{14}C]palmitate (specific activity 60.0 mCi/mmol) were obtained from GE Healthcare. Antibodies utilized included anti-(rabbit pNF-κBp65), anti-NF-κBp65, anti-fetuin-A, anti-adiponectin, anti-FAT (fatty acid translocase)/CD36 (cluster of differentiation 36), anti-aP2 (adipocyte protein 2), anti-PPARγ (peroxisome-proliferator-activated receptor γ) and anti-C/EBPβ antibodies were purchased from Santa Cruz Biotechnology. Alkaline-phosphatase-conjugated goat anti-rabbit secondary antibody was purchased from Sigma. Glucose estimation kit was procured from Autospan. Recombinant fetuin-A protein and a fetuin-A ELISA kit were procured from R&D Systems. Serum NEFA [non-esterified ('free') fatty acid] levels was measured by acyl-CoA synthase and acyl-CoA oxidase methods (Roche Diagnostics). All other chemicals were purchased from Sigma.

Cell lines and cell culture

The human hepatoma HepG2 and mouse pre-adipocyte 3T3-L1 cell lines were gifts from Dr Partha Banerjee, Georgetown University Medical Center, Washington, DC, U.S.A. The HepG2 cells were cultured in MEM (minimal essential medium) containing Earle's salts and non-essential amino acids supplemented with 2 mM L-glutamine, 1 mM sodium pyruvate, 10 % (v/v) FBS (fetal bovine serum), penicillin (100 units/ml) and streptomycin (100 μg/ml) in a humidified 5 % CO_2 atmosphere at 37 °C. 3T3-L1 pre-adipocytes were maintained in DMEM (Dulbecco's modified Eagle's medium) containing 10 % (v/v) FBS and antibiotics. When the cells reached confluence, they were cultured in ADM (adipocyte differentiation medium) containing DMEM supplemented with 10 % (v/v) FBS, 5 μg/ml insulin, 0.5 mmol/l 3-isobutyl-1-methylxanthine and 1 μmol/l dexamethasone.

Animal experiments

Adult male Sprague–Dawley rats weighing approx. 175–200 g were conditioned at 25 $\pm$ 2 °C with a 12 h light/12 h dark cycle and fed on a standard diet *ad libitum*. An insulin-resistant rat model was reared on an HFD (high-fat diet) for 12 weeks. In terms of total energy, the HFD consisted of 32.5 % lard, 32.5 % corn oil, 20 % sucrose and 15 % protein, whereas the standard diet contained 57.3 % carbohydrate, 18.1 % protein and 4.5 % fat. The energy content of the standard diet was 15 kJ/g and the HFD was 26 kJ/g. Control (C57BLKS/6J) and *db*/*db* [BKS.Cg-m$^{+/+}$ Lepr(db)/J, stock # 000642] mice obtained from the Jackson Laboratory aged 12–18 weeks were housed under a 12 h light/12 h dark cycle at 23 $\pm$ 2 °C (humidity 55 $\pm$ 5 %) with access *ad libitum* to food and water. Blood was collected from HFD-fed rats, *db*/*db* mice and their controls for the estimation of serum glucose, NEFA and fetuin-A levels. All animal experiments were performed following the guidelines prescribed by the Animal Ethics Committee.

Primary culture

Adult male Sprague–Dawley rats (weighing 175–200 g) were anaesthetized followed by opening of the abdomen. The liver was perfused via the portal vein by using modified Hanks medium. Perfused liver was isolated, minced and digested with type IV collagenase in original Hanks medium for 1 h at 37 °C. Digested cell suspension was filtered through two layers of nylon mesh and supernatant was removed. Cells were then resuspended in MEM supplemented with antibiotics (penicillin/streptomycin) and 0.2 % BSA. Viability of the cells was determined using the Trypan Blue exclusion method. Cells were plated in collagen-coated plates and cultured in a humidified 5 % CO_2 atmosphere at 37 °C.

Human subjects

Visceral adipose tissue was obtained from 12 patients (subjects without diabetes) who were admitted to the S.S.K.M. Hospital and underwent abdominal surgery. We obtained consent from all subjects included in the study and the approval of the ethical committee of the I.P.G.M. E&R, S.S.K.M. Hospital, Kolkata. Adipose tissue was rinsed with sterile 0.9 % NaCl solution. The tissue was then cleaned in HBSS (Hanks buffered saline solution) supplemented with 5.5 mM glucose. Adipose tissue was digested in HBSS containing 5.5 mM glucose, 5 % (w/v) FA-free BSA and 3.3 mg/ml type II collagenase for 30 min in a 37 °C water bath. The digestion mixture was passed through a tissue sieve. The pre-adipocyte-containing fraction was collected and washed several times by centrifugation at 585 ***g*** for 5 min. The supernatant was discarded, and the pellet containing pre-adipocytes was resuspended in standard medium consisting of DMEM supplemented with penicillin (100 units/ml) and streptomycin (100 μg/ml) and 10 % (v/v) FBS. Cells were plated in culture plates and kept in a humidified 5 % CO_2 atmosphere at 37 °C. For adipogenesis, the medium was further replaced by ADM.

Cell culture treatments

Confluent HepG2 cells were subcultured by trypsinization and subsequently seeded in six-well culture plates containing MEM with essential supplements. Cells were serum-starved for 24 h before starting the experiments. Lipid-containing media were prepared by conjugating lipid to BSA following our previously described method [17]. Confluent HepG2 cells were incubated for different periods (0, 2, 4, 6 and 8 h) or at different doses (0.25, 0.5, 0.75, 1.0 and 1.5 mM) in the absence or presence of palmitate. Cells were also incubated with different types of FAs (0.75 mM). When inhibitors were used, cells were pre-incubated with inhibitors such as SN-50 (50 μg/ml), actinomycin D (1 μM), cycloheximide (10 μM) or PDTC (pyrrolidine dithiocarbamate) (50 μM) for 1 h before treatment with palmitate. Rosiglitazone (10 μM) was co-incubated along with fetuin-A protein in pre-adipocytes. At the end of the incubation, medium was collected or cells were lysed and centrifuged at 10 000 ***g*** for 10 min and the supernatant was collected. The protein concentration of the supernatant and medium was determined by following the method described previously [18]. NF-κBp65 siRNA (short interfering RNA), C/EBPβ siRNA and pCMV-NF-κBp65 vector were transfected using Lipofectamine™ 2000 (Invitrogen) following

Table 1 Primers used in the present study

Primer	Direction	Sequence
NF-κBp65	Forward	5′-CCATCAGGGCAGATCTCAAACC-3′
	Reverse	5′-GCTGCTGAAACTCTGAGTTGTC-3′
Fetuin-A	Forward	5′-CCAGTGTCATTCCACCAGA-3′
	Reverse	5′-CGCAGCTATCACAAACTCCA-3′
C/EBPβ	Forward	5′-GGACGCAGCGGAGCCCGC-3′
	Reverse	5′-CTCGGCGGGCCACTGCTAG-3′
PPARγ	Forward	5′-ATCATCTACACGATGCTGGCC-3′
	Reverse	5′-CTCCCTGGTCATGAATCCTTG-3′
aP2	Forward	5′-TGATGCCTTTGTGGGAACCT-3′
	Reverse	5′-GCAAAGCCCACTCCCACTT-3′
CD36	Forward	5′-GAGCCATCTTTGAGCCTTCA-3′
	Reverse	5′-TCAGATCCGAACACAGCGTA-3′
IL-6	Forward	5′-ATTTCCTCTGGTCTTCTGGA-3′
	Reverse	5′-TCCTTAGCCACTCCTTCTGT-3′
TNFα	Forward	5′-TCTCAGCCTCTTCTCATTCC-3′
	Reverse	5′-ACTTGGTGGTTTGCTACGAC-3′
GAPDH	Forward	5′-GCCATCAACGACCCCTTC-3′
	Reverse	5′-AGCCCCAGCCTTCTCCA-3′

the manufacturer's protocol. 3T3-L1 and human pre-adipocytes were incubated with medium containing or not 1.5 mM Ca^{2+} in the presence of 100 μg/ml fetuin-A for 12 h followed by culture of cells in ADM. FITC-labelled fetuin-A was incorporated into adipocytes in the presence or absence of Ca^{2+}. Fetuin-A protein was FITC-labelled with the help of an FITC labelling kit (Calbiochem) following the manufacturer's protocol. Differentiated 3T3-L1 and primary adipocytes were stained with Oil Red O stain following the manufacturer's protocol (Cayman Chemical).

Western blots

Protein (50 μg) from cell lysates and media was resolved by SDS/PAGE (10 % gels) and transferred on to PVDF membranes (Millipore) using Semi-Dry Trans-Blot® Apparatus (Bio-Rad Laboratories). The membranes were first incubated with different primary antibodies at 1:1000 dilutions followed by goat anti-rabbit secondary antibody conjugated to alkaline phosphatase at the same dilutions using SNAP i.d.™ apparatus (Millipore). The protein bands were detected by using BCIP (5-bromo-4-chloroindol-3-yl phosphate)/NBT (Nitro Blue Tetrazolium).

RT (reverse transcription)–PCR and real-time PCR

Total RNA was extracted from different incubations using TRI Reagent (Sigma) according to the manufacturer's instructions. RT–PCR was performed using the Revert Aid™ first-strand cDNA synthesis kit (Fermentas Life Sciences). Alteration in gene expression was confirmed further by real-time PCR (Applied Biosystems). PCR was performed using gene-specific primers with the following reaction conditions: initial activation step at 95 °C for 15 min, then 40 cycles of denaturation at 95 °C for 30 s, annealing at 55 °C for 30 s and final extension at 72 °C for 30 s. *Gapdh* (glyceraldehyde-3-phosphate dehydrogenase) was simultaneously amplified in separate reactions. The C_t value was corrected using corresponding *Gapdh* controls. Primer sequences used were as shown in Table 1.

EMSA (electrophoretic mobility-shift assay)

EMSAs were performed using nuclear extracts prepared from different incubations with oligonucleotide probes specific for the NF-κB-binding site [wild–type, 5′-GCACCTGGGTTG-GTCCCGAAGC-3′; mutant, 5′-GCACCTGG**C**TTGGTCCC-GAAGC-3′ (mutated residue is in bold and underlined)] within the fetuin-A promoter. The probes were end-labelled with [γ-^{32}P]ATP with T4 polynucleotide kinase and then they were incubated with 10 μg of nuclear extracts in a 20 μl reaction volume for 45 min on ice. For the supershift assay, 2 μg of anti-NF-κBp65 antibody was added to the nuclear extract and the reaction mixture was resolved on a 5 % (w/v) polyacrylamide gel and visualized using a PhosphorImager (GE Healthcare).

ChIP (chromatin immunoprecipitation) assay

ChIP was performed using a ChIP assay kit (Upstate Biotechnology) following the manufacturer's protocol using anti-NF-κBp65 and anti-C/EBPβ antibodies. Primers used for amplification of human fetuin-A promoter sequence were 5′-CA-GAGCACCTGGTTGGT-3′ (forward) and 5′-GCCCCAGAG-CTGAGCAA-3′ (reverse), PCR products were resolved on an ethidium-bromide-stained 1.5 % agarose gel, and the image was captured by the Bio-Rad gel documentation system using Quantity One software.

[^{3}H]Leucine-incorporation study

HepG2 cells were serum-starved in KRP (Krebs–Ringer phosphate) buffer supplemented with 0.2 % BSA. To determine the rate of protein synthesis, serum-starved cells were incubated with 10 μCi/ml [^{3}H]leucine. Cells were incubated without or with palmitate or with palmitate plus actinomycin D. The medium was collected, and fetuin-A was pulled down using anti-fetuin-A antibody. Radioactive count was measured in a liquid scintillation counter (PerkinElmer Tri-Carb 2800TR).

[^{14}C]Palmitate uptake

Adipocytes transducted without or with fetuin-A were incubated with 1 μCi/ml [^{14}C]palmitate for 3 h. Cells were washed three times with ice-cold KRP buffer. Cells were solubilized with 1 % (v/v) NP-40 (Nonidet P40), and [^{14}C]palmitate was measured in a liquid scintillation counter.

[^{3}H]2-DOG uptake

Skeletal muscle tissue was dissected out from control and HFD-fed rats and *db*/*db* mice. The muscle tissue was washed thoroughly and subjected to digestion in DMEM in the presence of 0.02 % trypsin and 0.5 % collagenase for 30 min at 37 °C under 5 % CO_2. Isolated skeletal muscle cells and 3T3-L1 adipocytes were incubated in KRP buffer supplemented with 0.2 % BSA followed by 30 min of incubation in the presence of insulin (100 nM). [^{3}H]2-DOG (0.4 nmol/ml) was added to each incubation 5 min before the termination of incubation. Cells were washed three times with ice-cold KRP buffer in the presence of 0.3 mM phloretin. Cells were solubilized with 1 % NP-40 and [^{3}H]2-DOG was measured in a liquid scintillation counter.

Reporter assay

A pFetA-luc construct containing the 985 bp promoter region (chr3:187812685–187813673) of the human fetuin-A gene (GenBank®/EMBL accession number NM_001622) was purchased from SwitchGear Genomics. pFetA-luc served as a template for the generation of mutant plasmids with the help of the QuikChange® site-directed mutagenesis system (Stratagene). For mutated fetuin-A plasmid construction, sense oligonucleotides

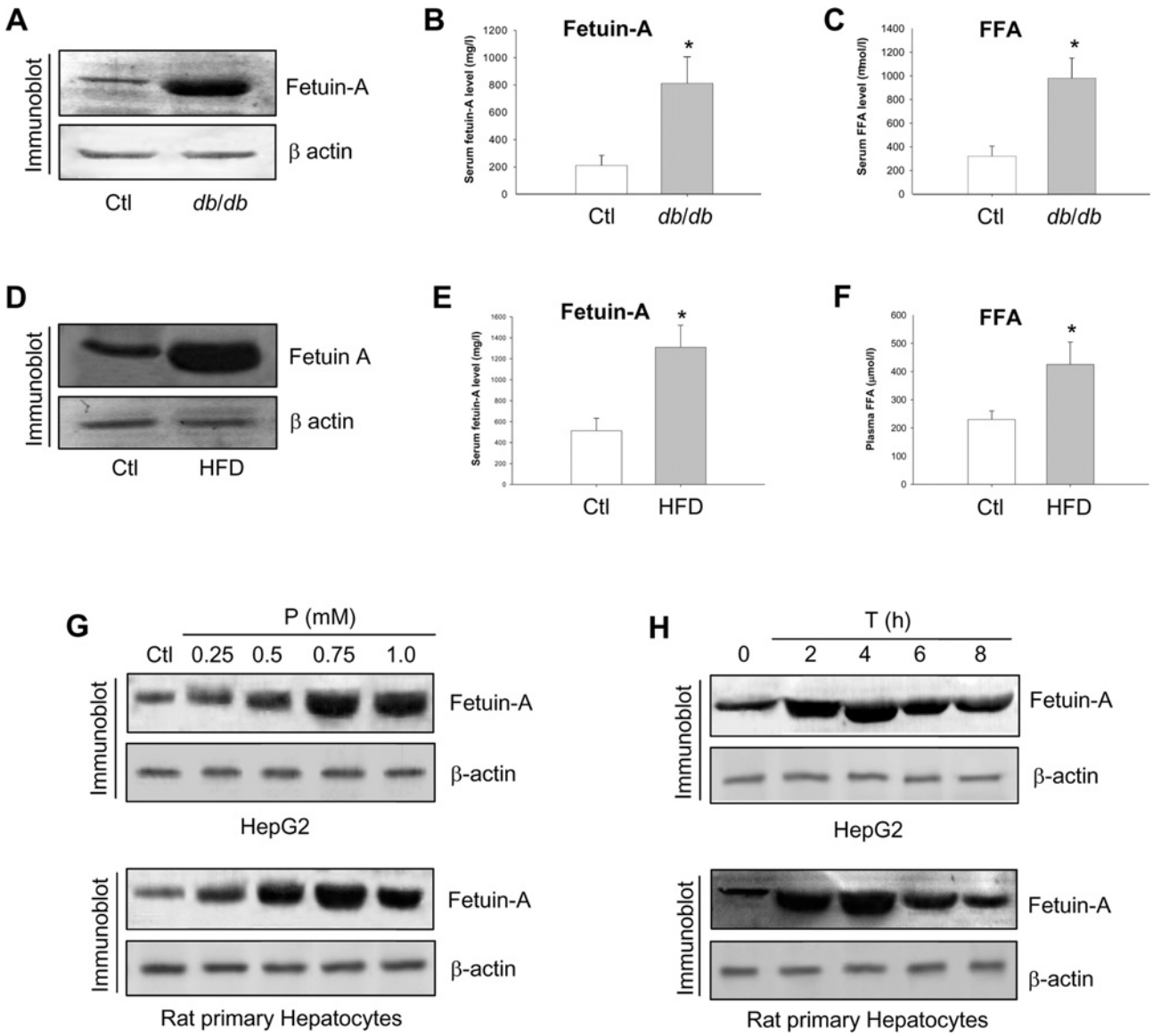

Figure 1 Interrelationship between FAs and fetuin-A

(**A**) Serum collected from control (Ctl) and *db*/*db* mice was subjected to immunoblot for fetuin-A. β-Actin was used as a loading control. (**B**) Serum fetuin-A levels were determined by ELISA. $^*P < 0.001$ compared with Ctl. (**C**) Serum NEFA ('FFA') levels were estimated from the above mice. Means $\pm$ S.E.M. were calculated from three experiments, with each experiment containing five control (Ctl) and five experimental animals. $^*P < 0.001$ compared with Ctl. (**D**) Serum fetuin-A levels in HFD-fed rats were measured by immunoblotting with anti-fetuin-A antibody. (**E**) Serum fetuin-A levels were estimated by ELISA. $^*P < 0.001$ compared with Ctl. (**F**) Estimation of serum NEFA ('FFA') levels in HFD-fed and control rats. $^*P < 0.001$ compared with Ctl. (**G**) HepG2 cells and rat primary hepatocytes were incubated with different concentrations of palmitate (P) for 4 h. On termination of incubations, medium was subjected to immunoblotting for fetuin-A. (**H**) The effect of palmitate (0.75 mM) on hepatocytes at different periods (T) was observed by Western blot analysis using an anti-fetuin-A antibody.

included oligohfetΔN1 (5′-AGGTCTGGAGAAGGAAGAGAACCCCACACGTT-3′), oligohfetΔN2 (5′-CCCACACGTTTTGCTCACCGTGGTCCTGCC-3′), oligohfetΔN3 (5′-CAAGAATCTTCCCCCAAAATCTTATACACATCTGTACCTTTGCT-3′), oligohfetΔN4 (5′-GATCACAGTAGAAGACCTGCCAAACCCATGGC-3′), oligohfetΔN5 (5′-GGTGTTTTTTTTTTTCTTTTGAACCACATCCTGTATCCTTATGCAATTCTTC-3′) and oligohfetΔN6 (5′-CTCTGGGGCAGCCTCGTCCTGCTCCT-3′) covering the deletion of fetuin-A $-251/-242$, $-277/-268$, $-395/-386$, $-559/-568$, $-794/-785$ and $-957/-948$ sequences respectively. HepG2 cells were transfected with wild-type or mutated pFetA-luc plasmid using Lipofectamine™ 2000. The luciferase activity was measured by the Steady-Glo luciferase assay system (Promega) following the manufacturer's instructions.

Statistical analysis

Data were analysed by one-way ANOVA where the F value indicated significance, means were compared by a post hoc multiple range test. All values are means $\pm$ S.E.M.

RESULTS

FA stimulates fetuin-A release by enhancing its gene expression

To have additional information on the association of lipid with fetuin-A, we selected *db*/*db* mice as it is a well known model for Type 2 diabetes with the hyperlipidaemic conditions and compared the serum profile with its control littermate. There was a significant ($P < 0.001$) increase in fetuin-A levels

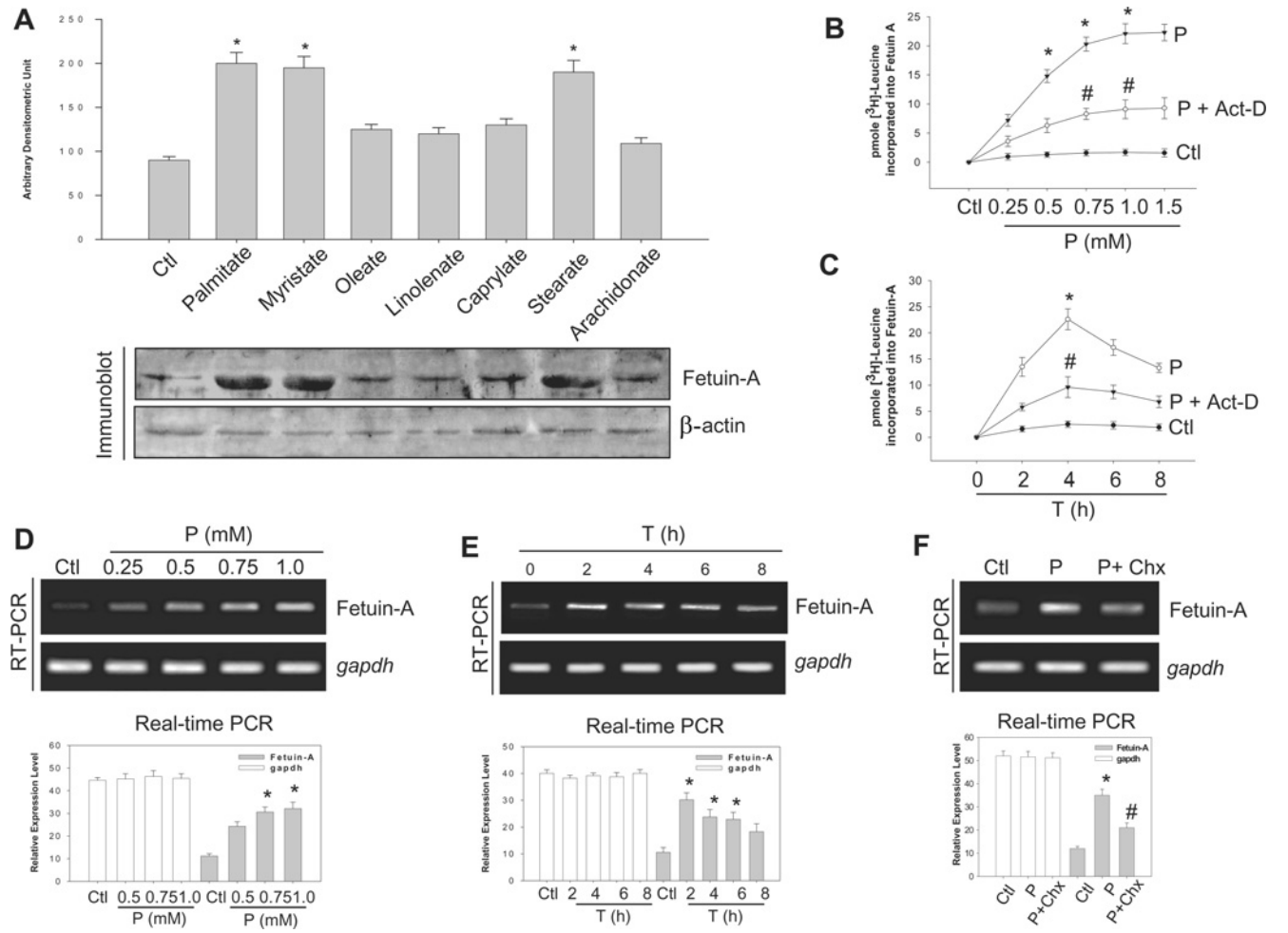

Figure 2 Effect of FAs on fetuin-A gene and protein expression

(**A**) HepG2 cells were incubated without (Ctl) or with different FAs (0.75 mM) for 4 h. On termination of incubations, medium was collected and subjected to immunoblot to determine fetuin-A. β-Actin served as an internal control. Means $\pm$ S.E.M. were calculated from four independent experiments. $^*P < 0.001$, compared with Ctl. (**B**) HepG2 cells were incubated in different concentrations of palmitate (P) in the presence of 10 μCi of [^{3}H]leucine without or with 1 μM actinomycin D (P+Act-D). Fetuin-A from the medium was pulled down by anti-fetuin-A antibody and processed for radioactive counting. (**C**) The same experiment was performed with hepatocytes incubated with 0.75 mM palmitate for different periods (T). Means $\pm$ S.E.M. were calculated from four independent experiments. $^*P < 0.001$, $^\#P < 0.001$, compared with Ctl. (**D**) HepG2 cells were incubated with different concentrations of palmitate (P). RNA extracted from the cells was subjected to RT–PCR and real-time PCR analysis using fetuin-A-specific primers taking *Gapdh* as an internal control. $^*P < 0.001$ compared with Ctl. (**E**) RNA extracted from HepG2 cells incubated with palmitate for different periods (T) was analysed by RT–PCR and real-time PCR. Means $\pm$ S.E.M. were calculated from three independent experiments. $^*P < 0.001$, compared with Ctl. (**F**) Effect of cycloheximide (Chx) on palmitate-incubated cells (P) was determined by RT–PCR and real-time PCR. Means $\pm$ S.E.M. were calculated from three independent experiments. $^*P < 0.001$, compared with Ctl; $^\#P < 0.01$, compared with P.

(Figures 1A and 1B) in *db*/*db* mice along with an increase in serum NEFAs (Figure 1C). We also investigated this in the HFD rat model where the significant increase in body weight (see Supplementary Figure S1A at http://www.BiochemJ.org/bj/429/bj4290451add.htm), blood glucose level (see Supplementary Figure S1B) and glucose uptake by skeletal muscle (see Supplementary Figure S1C) suggested development of insulin resistance. HFD-fed rats showed a similar trend of fetuin-A (Figures 1D and 1E) and NEFA (Figure 1F) levels to that observed in *db*/*db* mice. These findings suggest an association between FAs and fetuin-A. To have direct evidence, we incubated HepG2 cells and rat primary hepatocytes with palmitate. Consistent with *in vivo* observations, it was found that palmitate significantly increased fetuin-A secretion into the medium which was dose- (Figure 1G) and time- (Figure 1H) dependent. To observe whether all FAs are similarly involved in enhancing fetuin-A secretion, we incubated HepG2 cells with different FAs and results indicated that only long-chain saturated FAs were effective (Figure 2A). Since fetuin-A is a hepatic secretory protein, increased release could be related to its enhanced synthesis. To examine this, we incubated HepG2 cells with palmitate in the presence of [^{3}H]leucine and observed a significant elevation of fetuin-A protein synthesis ($P < 0.001$) which was inhibited by actinomycin D (Figures 2B and 2C). Palmitate strikingly up-regulated fetuin-A mRNA expression which was concentration- and time-dependent (Figures 2D and 2E). However, the palmitate augmentary effect was not direct as it was suppressed by cycloheximide (Figure 2F), indicating an involvement of a protein(s) mediator.

FA-induced fetuin-A synthesis is mediated through NF-κB

To search for this protein mediator, we considered NF-κB as a probable candidate because of its dependence on lipid for

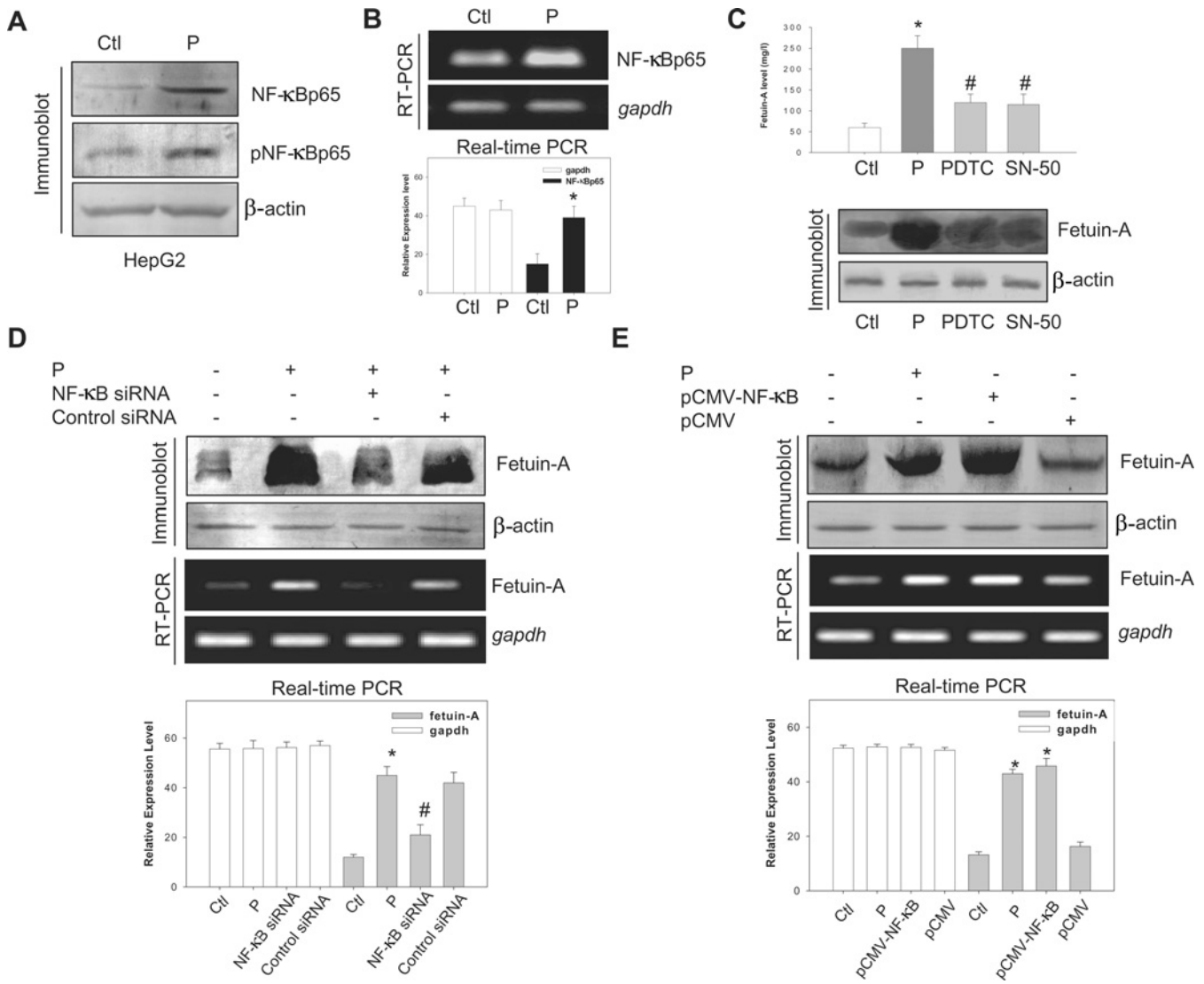

Figure 3 Palmitate stimulation of fetuin-A expression is mediated through NF-κB

(**A**) HepG2 cells were incubated without (Ctl) or with (P) 0.75 mM palmitate for 4 h. Cells were lysed and immunoblotted with anti-NF-κBp65 or anti-pNF-κBp65 antibodies. β-Actin served as an internal control. (**B**) RNA extracted from the above incubations was subjected to RT–PCR and real-time PCR using NF-κB-specific primers where *Gapdh* served as an internal control. Means $\pm$ S.E.M. were calculated from three independent experiments. $^*P < 0.001$, compared with Ctl. (**C**) HepG2 cells were incubated without (Ctl) or with (P) palmitate in the presence of PDTC or SN-50; fetuin-A released into the medium was determined by ELISA (upper panel) and immunoblot (lower panel). Means $\pm$ S.E.M. were calculated from four independent experiments. $^*P < 0.001$, compared with Ctl; $\#P < 0.001$, compared with P. (**D**) Control (Ctl) or NF-κB siRNA-transfected HepG2 cells were incubated with palmitate (P), and fetuin-A released into the medium was estimated by immunoblot analysis using an anti-fetuin-A antibody. RNA was extracted from the above mentioned incubated cells and subjected to RT–PCR and real-time PCR. (**E**) HepG2 cells were incubated without (Ctl) or with (P) palmitate or transfected with pCMV-NF-κBp65 or pCMV empty vector, and fetuin-A levels in the medium were determined by immunoblot analysis. RT–PCR and real-time PCR was performed with the RNA extracted from the above mentioned incubated cells. (**D** and **E**) Means $\pm$ S.E.M. were calculated from four independent experiments. $^*P < 0.001$, compared with Ctl; $\#P < 0.001$, compared with P.

its activation and nuclear translocation in liver cells [19,20]. In addition, we have recently reported an increase in NF-κB expression by palmitate that adversely affects insulin sensitivity [17]. Interestingly, palmitate also enhanced both NF-κB activity (Figure 3A) and expression (Figures 3A and 3B) in HepG2 cells and primary hepatocytes (see Supplementary Figures S2A and S2B at http://www.BiochemJ.org/bj/429/bj4290451add.htm). Palmitate stimulation of fetuin-A secretion from HepG2 cells could be attenuated by inhibitors of NF-κB, such as PDTC and SN-50 (Figure 3C), indicating that its effect on fetuin-A may be through NF-κB. We then checked whether alterations of NF-κB levels in HepG2 cells could be commensurate with fetuin-A synthesis. Transfection of NF-κB siRNA to HepG2 cells abrogated palmitate-induced fetuin-A protein and gene expression (Figure 3D). In contrast, forced expression of NF-κB in HepG2 cells enhanced fetuin-A protein and gene expression (Figure 3E) in the absence of palmitate. Considering that NF-κB may be up-regulating fetuin-A gene expression through the activation of the fetuin-A promoter, we performed a ChIP assay and found that NF-κB binding to the fetuin-A promoter was greatly enhanced due to palmitate, which was suppressed by SN-50 and NF-κB siRNA (Figure 4A, upper panel). Since salicylate has been shown to modulate the NF-κB pathway, we determined its effects on palmitate stimulation of NF-κB binding to the fetuin-A promoter

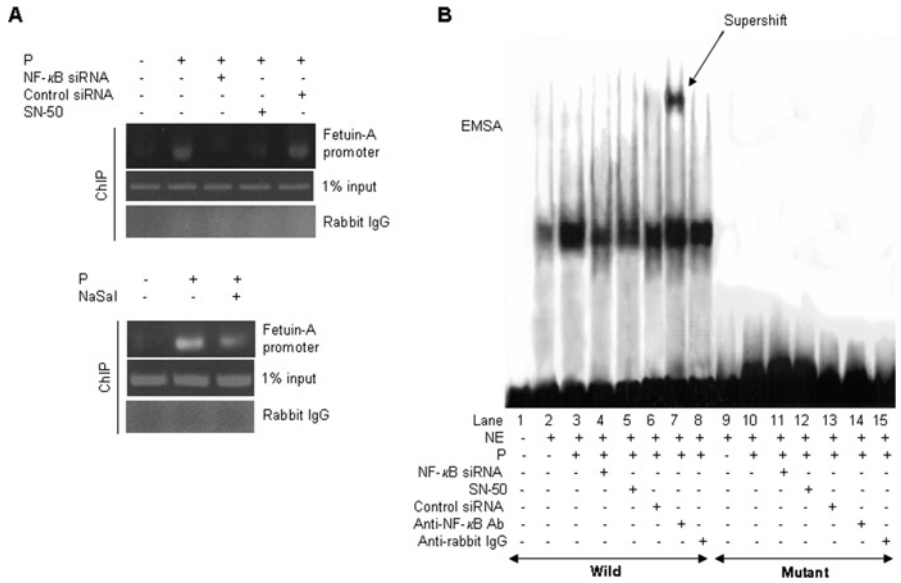

Figure 4 Palmitate-enhanced NF-κB binding to the fetuin-A promoter

(**A**) HepG2 cells transfected without or with NF-κB siRNA were incubated with palmitate (P) or with palmitate plus SN-50 (upper panel). HepG2 cells were incubated with palmitate or with palmitate plus sodium salicylate (NaSal) (lower panel). NF-κB binding to the fetuin-A promoter was determined by ChIP assay. (**B**) Nuclear extracts (NE) from the above mentioned incubated cells were subjected to EMSA. For the supershift assay, an anti-NF-κBp65 antibody was used. Mutant probe and non-specific anti-IgG antibody was used to determine specific binding of NF-κB on the fetuin-A promoter.

and found that salicylate inhibited the palmitate augmentary effect (Figure 4A, lower panel). We further confirmed it by EMSA, which showed that NF-κB binding activity increased in nuclear extract from palmitate-incubated cells, and the addition of anti-NF-κBp65 antibody supershifted the binding complex, indicating that this band constitutes the p65 subunit. To examine the specificity of the NF-κBp65–DNA interaction, we used a mutant oligonucleotide probe where binding activity was not observed (Figure 4B). These results demonstrate that palmitate stimulation of fetuin-A expression requires NF-κB.

Palmitate stimulation of fetuin-A promoter activity is NF-κB-dependent, but independent of C/EBPβ

To have better insight into the palmitate stimulation of fetuin-A through NF-κB, there is a need to demonstrate regulation of the fetuin-A promoter activity by NF-κB and to detect specific NF-κB-binding sites on the fetuin-A promoter, and then whether the occupation of those sites by NF-κB could activate the promoter. To achieve these objectives, we transfected pFetA-Luc vector to HepG2 cells, co-transfected HepG2 cells with NF-κB siRNA followed by palmitate incubation or transfected HepG2 cells with pCMV-NF-κBp65 vector and then incubated them in the absence of palmitate. Palmitate enhanced fetuin-A reporter activity which was significantly attenuated in NF-κB-knockout cells, whereas reporter activity markedly increased in cells transfected with pCMV-NF-κBp65 in the absence of palmitate. Interestingly, salicylate which is an inhibitor of NF-κB activity, also reduced luciferase activity indicating this to be a reflection of reduced NF-κB binding to the fetuin-A promoter (Figure 5A). Hence, palmitate regulation of fetuin-A expression is NF-κB-dependent; once the critical concentration of NF-κB within the cell is achieved, fetuin-A up-regulation may occur in the absence of palmitate. We then searched for NF-κB-binding sites on the fetuin-A promoter. There are six putative binding sites (termed N1, N2, N3, N4, N5 and N6) as detected by using the Match computer program with a sequence homology with classical NF-κB-response elements (see Supplementary Table S1 at http://www.BiochemJ.org/bj/429/bj4290451add.htm). To investigate whether these elements were involved in fetuin-A promoter activation due to NF-κB, we transfected wild-type and mutated pFetA-Luc vector construct into HepG2 cells and incubated them with palmitate. Constructs lacking N1, N4 or N5 but containing N2, N3 or N6 increased luciferase activity due to palmitate, whereas deletion of N2, N3 or N6 abolished reporter gene activity (Figure 5B). Furthermore, luciferase activity was attenuated in NF-κB-silenced HepG2 cells transfected with pN2-N3-N6-FetA-Luc construct; this was reversed in NF-κB-overexpressed cells (Figure 5C). Therefore N2, N3 and N6 elements are essential for palmitate-induced NF-κB-mediated fetuin-A promoter activation. On finding evidence in favour of palmitate stimulation of fetuin-A promoter activation due to NF-κB binding, we considered whether C/EBPβ has any association with the palmitate stimulatory effect on the fetuin-A promoter as glucocorticoid up-regulates fetuin-A through C/EBPβ. The fetuin-A promoter has several binding sites for C/EBPβ, and occupation of them augmented fetuin-A expression [16]. However, palmitate did not alter C/EBPβ binding to the fetuin-A promoter (Figure 5D); it also had no effect on C/EBPβ expression (Figure 5E) or fetuin-A protein and gene expression in C/EBPβ-knockout cells (Figure 5F). Moreover, NF-κB- and C/EBPβ-binding sites on the fetuin-A promoter are different. These findings suggest that, in lipid-induced up-regulation of fetuin-A, NF-κB plays the role of a mediator, whereas C/EBPβ remains uninvolved.

Impairment of adipocyte function by fetuin-A

On studying the mechanism of lipid-induced regulation of fetuin-A synthesis in liver cells, we wondered whether such robust expression of fetuin-A could only be attributed to its known adverse effects on the phosphorylation of insulin receptor tyrosine

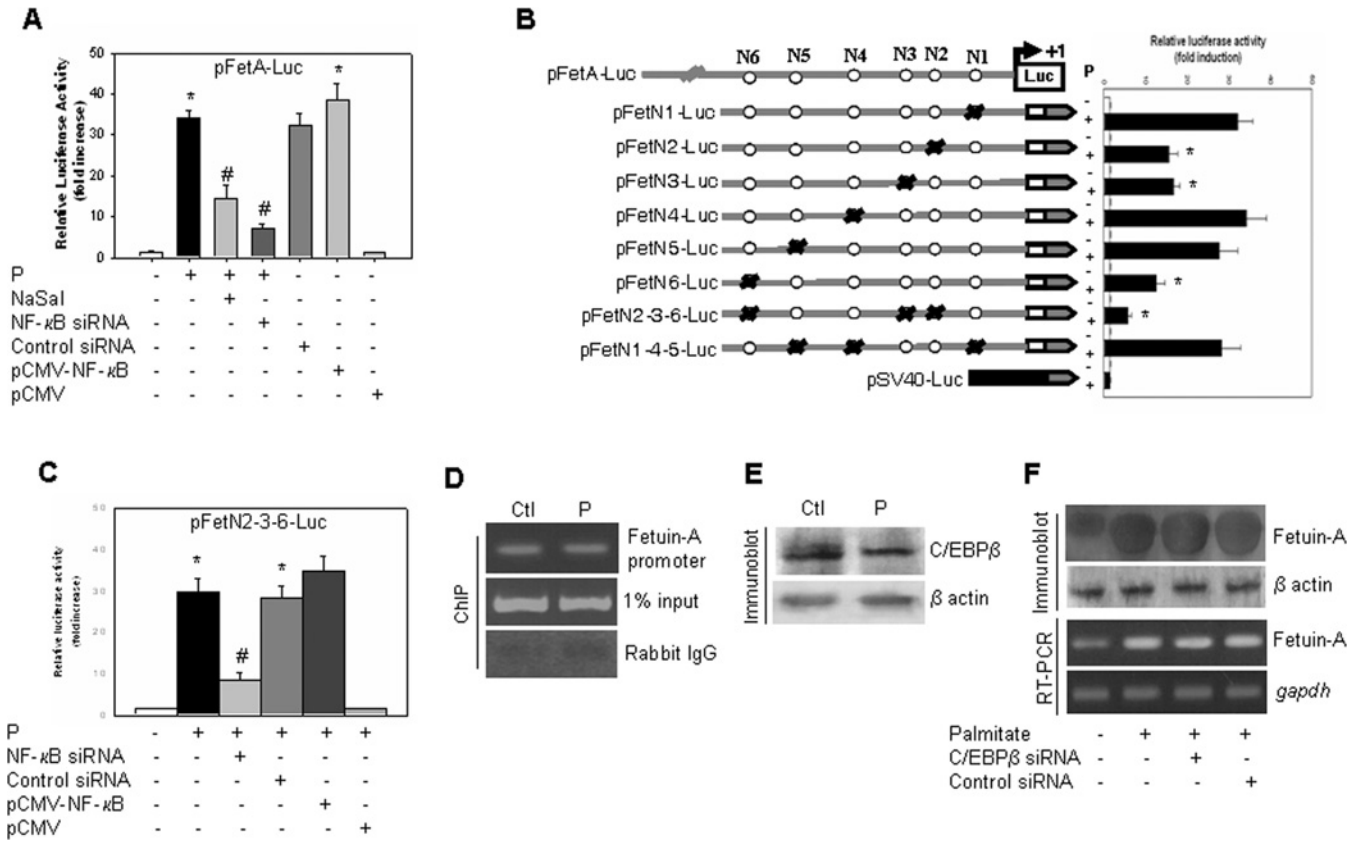

Figure 5 Increase in fetuin-A promoter activity by NF-κB

(**A**) pFetA-luc-transfected HepG2 cells or HepG2 cells co-transfected with NF-κB siRNA or pCMV-NF-kBp65 vector were incubated with palmitate (P) or palmitate plus sodium salicylate (P+NaSal). On termination of incubations, reporter activity was determined by using luciferase assay. Means $\pm$ S.E.M. were calculated from three independent experiments. *$P < 0.001$, compared with Ctl; #$P < 0.001$, compared with P. (**B**) A cartoon shows pFetA-luc vector with the six putative NF-κB-binding elements (N1, N2, N3, N4, N5 and N6). On the right-hand side, luciferase activity of palmitate-incubated HepG2 cells transfected with mutated pFetA-luc vector demonstrates the requirement of N2, N3 and N6 for its activity. (**C**) Luciferase activity was also observed in cells transfected with pN2-N3-N6-FetA-luc construct or co-transfected with NF-κB siRNA or pCMV-NF-κBp65. Means $\pm$ S.E.M. were calculated from five independent experiments. *$P < 0.001$, compared with Ctl; #$P < 0.001$, compared with P. (**D**) HepG2 cells were incubated without (Ctl) or with (P) palmitate and subjected to ChIP assay using an anti-C/EBPβ antibody. (**E**) HepG2 cells were incubated without (Ctl) or with palmitate (P) and immunoblotted for C/EBPβ. β-Actin was used as an internal control. (**F**) HepG2 cells transfected with C/EBPβ siRNA was incubated without or with palmitate (P) and immunoblotted with an anti-fetuin-A antibody or subjected to RT–PCR using fetuin-A-specific primers.

kinase or could it also target other impairments associated with insulin resistance and Type 2 diabetes. A few reports directed our attention towards adipocytes. It is reported that when fetuin-A-null mice were fed on an HFD, there is a significant decrease in body fat, and they are resistant to weight gain [6]. These results imply that the presence of fetuin-A would promote fat accumulation. In haemodialysis patients, fetuin-A is associated with truncal obesity and dyslipidaemia [21]. Moreover, an anti-diabetic thiazolidinedione class of drug, known for its plasma NEFA-reducing effect, also decreased fetuin-A [22]. We therefore considered adipocytes to be another target and examined the role of fetuin-A on adipocyte function. Fetuin-A uptake in cells has been shown to be Ca^{2+}-dependent [23,24]. We utilized this information to determine whether fetuin-A acts from the outside or whether its entry into the cell is obligatory. Our experiments therefore included adipocyte incubations with or without 1.5 mM Ca^{2+} (less than the normal circulatory level [25]). Interestingly, fetuin-A was readily translocated into the cells in the presence of Ca^{2+} (Figure 6A). Since Ca^{2+} remains bound to albumin in circulation, determination of the level of free Ca^{2+} that permitted maximum uptake of fetuin-A is important. We have found that 1.5 mM $CaCl_2$ produced 0.25 μM free ionized Ca^{2+} in adipocytes which induced maximum fetuin-A entry into the cells, whereas 2 mM $CaCl_2$ resulting in 0.28 μM free Ca^{2+} in cells had no additional effect on fetuin-A entry (see Supplementary Figures S3A and S3B at http://www.BiochemJ.org/bj/429/bj4290451add.htm). These results suggest 0.25 μM free Ca^{2+} as the threshold level for permeating fetuin-A entry. We transducted fetuin-A to mouse 3T3-L1 and human pre-adipocytes and traced its activity in differentiated adipocytes by culturing them in ADM followed by the determination of lipid content with the help of Oil Red O staining. There was a significant reduction in lipid droplet size and numbers (Figure 6B) and diminished lipid content (Figure 6C) due to fetuin-A in both cases. In contrast, rosiglitazone, a PPARγ agonist, increased lipid accumulation, which was substantially reduced by fetuin-A (Figures 6B and 6C). That uptake of lipid by adipocytes is impaired due to fetuin-A was observed with [^{14}C]palmitate, and it was found that addition of fetuin-A to 3T3-L1 incubation significantly inhibited [^{14}C]palmitate uptake (Figure 6D).

We examined fetuin-A's effect on PPARγ, a well-known adipogenic factor [26,27] and observed a significant reduction in its protein (Figure 7A) and gene (Figure 7B) expression in fetuin-A-treated cells. We then checked the protein and gene expressions

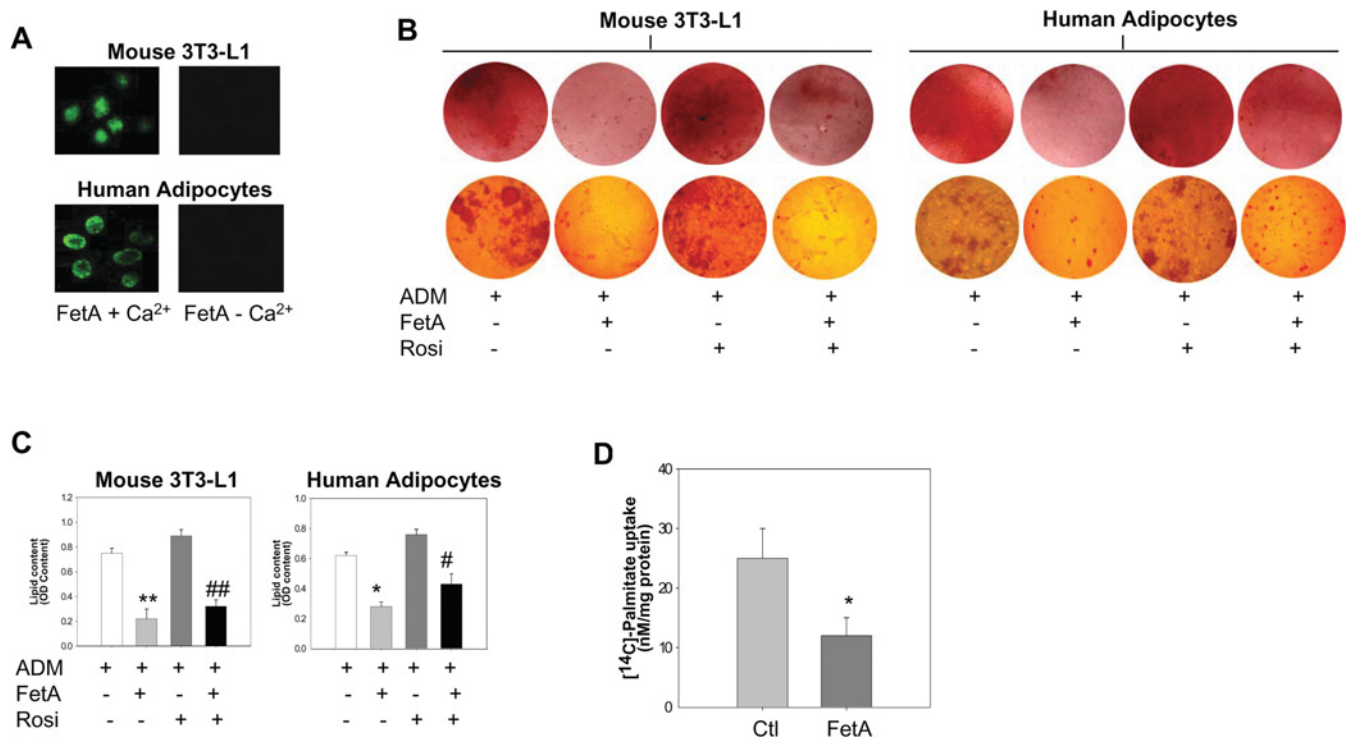

Figure 6 Fetuin-A impairs adipocyte function

(**A**) FITC-conjugated fetuin-A (FetA) was incubated with mouse 3T3-L1 and human adipocytes in the absence or presence of Ca^{2+}. (**B**) Mouse 3T3-L1 and human adipocytes were incubated with or without fetuin-A (FetA) or co-incubated with rosiglitazone (Rosi) in ADM. Adipogenic differentiation was measured by Oil Red O staining (upper panel) and were observed under microscopy (lower panel). (**C**) Lipid content was determined by the dye-extraction method. Means ± S.E.M. were calculated from four independent experiments. $^{**}P < 0.001$, $^{*}P < 0.01$ compared with ADM; $\#\#P < 0.001$, $\#P < 0.01$ compared with ADM+Rosi. (**D**) 3T3-L1 adipocytes were incubated with [^{14}C]palmitate (Ctl) or [^{14}C]palmitate plus fetuin-A (FetA) followed by the determination of the radioactive count from cell lysates. Means ± S.E.M. were calculated from five independent experiments. $^{*}P < 0.01$, compared with Ctl.

of downstream molecules of PPARγ such as adiponectin, aP2 and FAT/CD36 (Figures 7A and 7B) and found all of them to be down-regulated by fetuin-A. Fetuin-A imposed defects on adipocytes were also indicated by the up-regulation of TNFα (tumour necrosis factor α) and IL-6 (interleukin 6) (Figures 7A and 7B). Presumably, all of these would inflict a severe damage to adipocyte function and thereby cause insulin resistance, which is evident from the inhibition of insulin-stimulated [^{3}H]2-DOG uptake and GLUT4 (glucose transporter 4) translocation (Figure 7C).

DISCUSSION

On the basis of the reports that have accumulated for the last several years, it is reasonable to consider fetuin-A as an important factor associated with insulin resistance and Type 2 diabetes. The fetuin-A gene is expressed in the liver and the protein, once synthesized, is immediately secreted into the circulation; its high level is linked to impairment of insulin sensitivity in animals and humans [1–3]. One site of its action is known: it adversely affects the insulin receptor tyrosine kinase and that inhibits insulin-stimulated downstream signalling [4–6]. However, certain important aspects still remain unclear. (i) It is not known which factor(s) regulates up-regulation of fetuin-A. Glucocorticoid is known to induce fetuin-A gene expression through the activation of its promoter by C/EBPβ. FA's role on insulin resistance is well known [28–31], therefore whether its effect is mediated through the same pathway requires investigation. (ii) On the other hand, involvement of lipid has been implicated in the increase in fetuin-A by many [11–13], which is logical as lipid is known to cause insulin resistance. However, how lipid influences fetuin-A up-regulation is unclear, as there is no direct evidence in favour of this. (iii) During insulin resistance and Type 2 diabetes, consistently high levels of fetuin-A indicate an alternative target(s) of fetuin-A besides its classical effect on insulin receptor tyrosine kinase, and a couple of recent reports suggested defects in adipogenesis [3,21]. This is pertinent as it would enhance FA levels and that in turn will adversely affect insulin sensitivity. However, here also clearer evidence is required to show that fetuin-A is anti-adipogenic. In the present study, we wanted to add new information, which may fill some gaps in our understanding of fetuin-A's regulation during insulin resistance.

We first set our examination on *in vivo* insulin-resistant and Type 2 diabetes models, as results from these experiments would indicate the nature of the relationship between lipid and fetuin-A. The ideal model is *db*/*db* mice, and in them it is clearly observed that a significant increase in NEFA circulatory levels coexisted with high levels of fetuin-A. A similar observation was made with HFD-fed rats. Taking this cue as meaningful, we performed experiments with the human liver cell line HepG2 and rat primary hepatocytes. In both cell culture systems, the type of results obtained are fairly uniform in nature, both depicted enhancement of fetuin-A expression to more than 4-fold in comparison with control. However, the palmitate effect is not direct; it is mediated through NF-κB. Our earlier observations on lipid-induced overexpression of NF-κB in insulin target cells [20] led us to presume that, since NF-κB is known to be involved

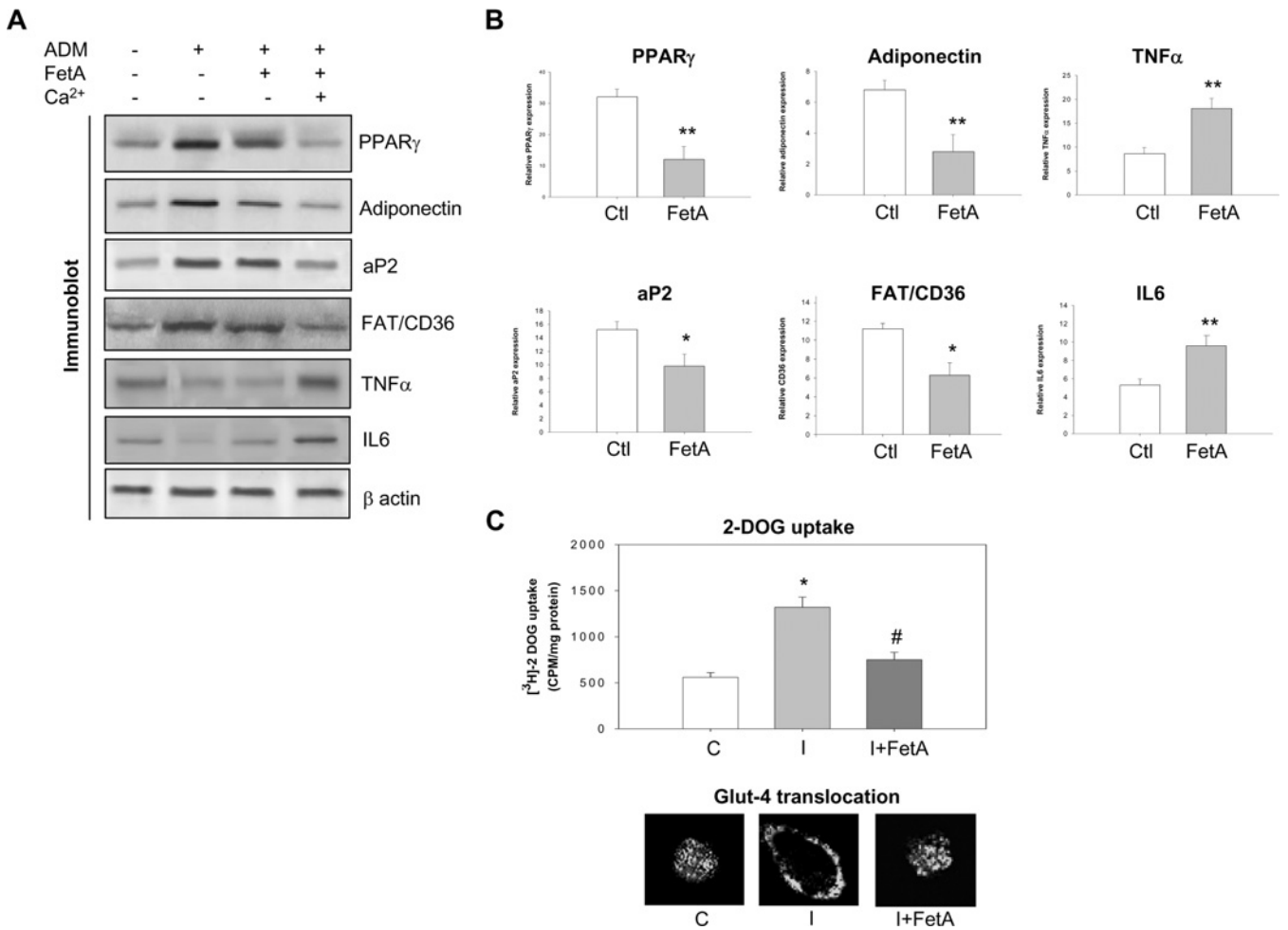

Figure 7 Fetuin-A down-regulates adipogenic factors and stimulates pro-inflammatory cytokines

(**A**) 3T3-L1 adipocytes were incubated with fetuin-A in the absence or presence of Ca^{2+} in ADM. Adiponectin, TNFα or IL-6 released in the medium was estimated by immunoblot analysis using anti-adiponectin, anti-TNFα and anti-IL-6 antibodies respectively. Cell lysates from different incubations were subjected to Western blot analysis using anti-PPARγ, anti-aP2 and anti-FAT/CD36 antibodies. β-Actin served as an internal control. (**B**) 3T3-L1 adipocytes were incubated without (Ctl) or with fetuin-A (FetA) in the presence of Ca^{2+} (1.5 mM). On termination of incubation, RNA was extracted and subjected to real-time PCR by using gene-specific primers of PPARγ, adiponectin, TNFα, aP2, FAT/CD36 and IL-6. Means $\pm$ S.E.M. were calculated from three independent experiments. $^*P < 0.01$, $^{**}P < 0.001$, compared with Ctl. (**C**) Fetuin-A-transducted 3T3-L1 adipocytes were incubated with insulin followed by [^{3}H]2-DOG. 2-DOG uptake by the cells was determined by radioactive count (upper panel). $^*P < 0.01$, compared with Ctl; $\#\ P < 0.01$ compared with I+FetA. GFP (green fluorescent protein)–GLUT4 plasmid-transfected 3T3-L1 adipocytes were incubated with insulin in the absence or presence of fetuin-A, and GLUT4 translocation was observed by confocal microscopy (lower panel).

in insulin resistance, its greater turnover and activity may be a causative factor in up-regulating fetuin-A. FA has been shown to activate NF-κB and its nuclear translocation compromised insulin sensitivity in insulin target cells [18,19]. Here also, palmitate elevated fetuin-A through a similar pathway, it increases fetuin-A promoter activity through the enhancement of NF-κB binding that significantly augmented fetuin-A gene and protein expression. Interestingly, it is not palmitate alone, but a few other long-chain FAs that are associated in fetuin-A expression as shown in the present study and these FAs also mediate their effect through NF-κB (results not shown). We used several specific inhibitors to block NF-κB, and all of them reduced palmitate-induced increased expression of fetuin-A in HepG2 cells. Since several authors have indicated salicylate to be an inhibitor of NF-κB activity [32,33], we also found that salicylate inhibited palmitate stimulation of NF-κB binding to the fetuin-A promoter which reduces promoter activity. Our findings support the validity of earlier reports on fetuin-A in diabetic patients and animals where it has been retained consistently at high levels in the serum [2,3,13].

Another interesting observation is the identification of NF-κB-response elements on the fetuin-A promoter. Since it is known that glucocorticoids induce up-regulation of fetuin-A expression through C/EBPβ [16], we examined the effect of palmitate on C/EBPβ and did not find any alteration of C/EBPβ expression or activity. This suggests that C/EBPβ is not involved in palmitate-induced fetuin-A up-regulation. To have a better insight, we searched for NF-κB-binding sites on the fetuin-A promoter and found that, out of six binding sites, three are responsible for fetuin-A promoter activation and these are different from what was reported in the case of C/EBPβ. Hence, it appears that FA takes a separate pathway in up-regulating fetuin-A expression which corroborates the condition that prevails during insulin resistance.

On studying the mechanism of lipid-induced regulation of fetuin-A synthesis in liver cells, we thought that this high expression of fetuin-A may not only be for its inhibition of insulin

receptor tyrosine kinase phosphorylation, but also possibly target other impairments associated with insulin resistance and Type 2 diabetes. At this juncture, two reports attracted our attention, one demonstrated that fetuin-A-null mice are protected against HFD-induced obesity [6] and another showed a decrease in adiponectin levels in adipocytes due to fetuin-A [15]. These reports suggest adipocytes to be another target of fetuin-A. We therefore expected that fetuin-A will inflict defects on adipocyte function. Our observation with both human and 3T3-L1 adipocytes demonstrated that fetuin-A effects several impairments, which abrogates uptake of lipid into the cells. Pro-adipogenic function of PPARγ, adiponectin, FAT/CD36 and aP2 are known, and all of them are down-regulated by fetuin-A. All these direct to a reasonable notion that such impairments may cause obesity and insulin resistance. Association of lipid and NF-κB with insulin resistance and Type 2 diabetes is well known, it is also fairly well known that fetuin-A is linked to insulin resistance. However, a connection between lipid, NF-κB and fetuin-A leading to the impairment of adipocyte function is not known. Our present work has contributed in understanding these shaded areas and pointed out that this pathway may serve as a novel therapeutic target for insulin resistance and Type 2 diabetes.

AUTHOR CONTRIBUTION

Suman Dasgupta and Sushmita Bhattacharya designed and conducted experiments, and co-wrote the paper. Anindita Biswas conducted the experiments on HFD-fed rats, Subeer Majumdar conducted experiments on *db*/*db* mice and co-wrote the paper. Satinath Mukhopadhyay evaluated results and co-wrote the paper. Sukanta Ray performed human adipocyte experiments. Samir Bhattacharya designed experiments, supervised the study, evaluated the results, and co-wrote the paper.

ACKNOWLEDGEMENTS

We thank Dr Partha P. Banerjee (Georgetown University Medical Center, Washington, DC, U.S.A.) for providing HepG2, 3T3-L1 cell lines and pCMV-NF-κBp65 vector, Dr Jeffrey E. Pessin (Albert Einstein College of Medicine, New York, NY, U.S.A.) for the GFP–GLUT4 vector and the Head of Department of Zoology, Visva-Bharati University, for extending the facilities required for the present investigation. We deeply appreciate the help of Professor Shelley Bhattacharya, Visva-Bharati University, and Dr Gaurangi Maitra, Tezpur University, Tezpur, India, for correcting grammatical errors and improving the quality of the writing before submission.

FUNDING

This work was supported by the Department of Science and Technology of the Ministry of Science and Technology, New Delhi [grant number VI-D&P/137/06-07/TDT]. S.D. expresses his gratitude to the University Grants Commission, New Delhi, for the award of Research Fellowship.

REFERENCES

1 Stefan, N., Fritsche, A., Weikert, C., Boeing, H., Joost, H. G., Haring, H. U. and Schulze, M. B. (2008) Plasma fetuin-A levels and the risk of type 2 diabetes. Diabetes **57**, 2762–2767
2 Mori, K., Emoto, M., Yokoyama, H., Araki, T., Teramura, M., Koyama, H., Shoji, T., Inaba, M. and Nishizawa, Y. (2006) Association of serum fetuin-A with insulin resistance in type 2 diabetic and nondiabetic subjects. Diabetes Care **29**, 468
3 Ix, J. H., Wassel, C. L., Kanaya, A. M., Vittinghoff, E., Johnson, K. C., Koster, A., Cauley, J. A., Harris, T. B., Cummings, S. R. and Shlipak, M. G. (2008) Fetuin-A and incident diabetes mellitus in older persons. JAMA, J. Am. Med. Assoc. **300**, 182–188
4 Auberger, P., Falquerho, L., Contreres, J. O., Pages, G., Le Cam, G., Rossi, B. and Le Cam, A. (1989) Characterization of a natural inhibitor of the insulin receptor tyrosine kinase: cDNA cloning, purification, and anti-mitogenic activity. Cell **58**, 631–640
5 Rauth, G., Pöschke, O., Fink, E., Eulitz, M., Tippmer, S., Kellerer, M., Häring, H. U., Nawratil, P., Haasemann, M., Jahnen-Dechent, W. and Müller-Esterl, W. (1992) The nucleotide and partial amino acid sequences of rat fetuin: identity with the natural tyrosine kinase inhibitor of the rat insulin receptor. Eur. J. Biochem. **204**, 523–529
6 Mathews, S. T., Singh, G. P., Ranalletta, M., Cintrón, V. J., Qiang, X., Goustin, A. S., Jen, K. L., Charron, M. J., Jahnen-Dechent, W. and Grunberger, G. (2002) Improved insulin sensitivity and resistance to weight gain in mice null for the *Ahsg* gene. Diabetes **51**, 2450–2458
7 Srinivas, P. R., Wagner, A. S., Reddy, L. V., Deutsch, D. D., Leon, M. A., Goustin, A. S. and Grunberger, G. (1993) Serum α_2-HS-glycoprotein is an inhibitor of the human insulin receptor at the tyrosine kinase level. Mol. Endocrinol. **7**, 1445–1455
8 Grunberger, G. M. S., Mathews, S. T. and Deutsch, D. D. (2002) Tyrosine kinase inhibitors. In Insulin Signaling: from Cultured Cells to Animal Models (Grunberger, G. M. S. and Zick, Y., eds), pp. 281–298, Taylor and Francis, New York
9 Mathews, S. T., Rakhade, S., Zhou, X., Parker, G. C., Coscina, D. V. and Grunberger, G. (2006) Fetuin null mice are protected against obesity and insulin resistance associated with aging. Biochem. Biophys. Res. Commun. **350**, 437–443
10 Vionnet, N., Hani, E. H., Dupont, S., Gallina, S., Francke, S., Dotte, S., De Matos, F., Durand, E., Leprêtre, F., Lecoeur, C. et al. (2000) Genomewide search for type 2 diabetes-susceptibility genes in French whites: evidence for a novel susceptibility locus for early-onset diabetes on chromosome 3q27-qter and independent replication of a type 2-diabetes locus on chromosome 1q21-q24. Am. J. Hum. Genet. **67**, 1470–1480
11 Kelley, D. E., McKolanis, T. M., Hegazi, R. A., Kuller, L. H. and Kalhan, S. C. (2003) Fatty liver in type 2 diabetes mellitus: relation to regional adiposity, fatty acids, and insulin resistance. Am. J. Physiol. Endocrinol. Metab. **285**, 906–916
12 Stefan, N., Hennige, A. M., Staiger, H., Machann, J., Schick, F., Krober, S. M., Machicao, F., Fritsche, A. and Haring, H. U. (2006) α_2-Heremans–Schmid glycoprotein/fetuin-A is associated with insulin resistance and fat accumulation in the liver in humans. Diabetes Care **29**, 853–857
13 Lin, X., Braymer, H. D., Bray, G. A. and York, D. A. (1998) Differential expression of insulin receptor tyrosine kinase inhibitor (fetuin) gene in a model of diet-induced obesity. Life Sci. **63**, 145–153
14 Dahlman, I., Eriksson, P., Kaaman, M., Jiao, H., Lindgren, C. M., Kere, J. and Arner, P. (2004) α_2-Heremans–Schmid glycoprotein gene polymorphisms are associated with adipocyte insulin action. Diabetologia **47**, 1974–1979
15 Hennige, A. M., Staiger, H., Wicke, C., Machicao, F., Fritsche, A., Häring, H. U. and Stefan, N. (2008) Fetuin-A induces cytokine expression and suppresses adiponectin production. PLoS ONE **3**, e1765
16 Wöltje, M., Tschöke, B., Bülow, V., Westenfeld, R., Denecke, B., Gräber, S. and Jahnen-Dechent, W. (2006) CCAAT enhancer binding protein β and hepatocyte nuclear factor 3β are necessary and sufficient to mediate dexamethasone-induced up-regulation of α_2 HS glycoprotein/fetuin-A gene expression. J. Mol. Endocrinol. **36**, 261–277
17 Barma, P., Bhattacharya, S., Bhattacharya, A., Kundu, R., Dasgupta, S., Biswas, A., Bhattacharya, S., Roy, S. S. and Bhattacharya, S. (2009) Lipid induced overexpression of NF-κB in skeletal muscle cells is linked to insulin resistance. Biochim. Biophys. Acta **1792**, 190–200
18 Lowry, O. H., Rosebrough, N. J., Farr, A. E. and Randall, R. J. (1951) Protein measurement with Folin phenol reagent. J. Biol. Chem. **193**, 265–275
19 Boden, G., She, P., Mozzoli, M., Cheung, P., Gumireddy, K., Reddy, P., Xiang, X., Luo, Z. and Ruderman, N. (2005) Free fatty acids produce insulin resistance and activate the proinflammatory nuclear factor-κB pathway in rat liver. Diabetes **54**, 3458–3465
20 Cai, D., Yuan, M., Frantz, D. F., Melendez, P. A., Hansen, L., Lee, J. and Shoelson, S. E. (2005) Local and systemic insulin resistance resulting from hepatic activation of IKK-β and NF-κB. Nat. Med. **11**, 183–190
21 Chen, H. Y., Chiu, Y. L., Hsu, S. P., Pai, M. F., Lai, C. F., Peng, Y. S, Kao, T. W., Hung, K. Y., Tsai, T. J. and Wu, K. D. (2009) Association of serum fetuin-A with truncal obesity and dyslipidemia in non-diabetic hemodialysis patients. Eur. J. Endocrinol. **160**, 777–783
22 Mori, K., Emoto, M., Araki, T., Yokoyama, H., Lee, E., Teramura, M., Koyama, H., Shoji, T., Inaba, M. and Nishizawa, Y. (2008) Effects of pioglitazone on serum fetuin-A levels in patients with type 2 diabetes mellitus. Metab. Clin. Exp. **57**, 1248–1252
23 Chen, N. X., O'Neill, K. D., Chen, X., Duan, D., Wang, E., Sturek, M. S., Edwards, J. M. and Moe, S. M. (2007) Fetuin-A uptake in bovine vascular smooth muscle cells is calcium dependent and mediated by annexins. Am. J. Physiol. Renal Physiol. **292**, F599–F606
24 Mellgren, R. L. and Huang, X. (2007) Fetuin-A stabilizes m-calpain and facilitates plasma membrane repair. J. Biol. Chem. **282**, 35868–35877
25 Fuszek, P., Lakatos, P., Tabak, A., Papp, J., Nagy, Z., Takacs, I., Horvath, H. C., Lakatos, P. L. and Speer, G. (2004) Relationship between serum calcium and CA 19–9 levels in colorectal cancer. World J. Gastroenterol. **10**, 1890–1892
26 Tontonoz, P., Hu, E. and Spiegelman, B. M. (1994) Stimulation of adipogenesis in fibroblasts by PPARγ2, a lipid-activated transcription factor. Cell **79**, 1147–1156
27 Farmer, S. R. (2005) Regulation of PPARγ activity during adipogenesis. Int. J. Obes. **29**, S13–S16

28 Boden, G. (1997) Role of fatty acids in the pathogenesis of insulin resistance and NIDDM. Diabetes **46**, 3–10
29 Santomauro, A. T., Boden, G., Silva, M. E., Rocha, D. M., Santos, R. F., Ursich, M. J., Strassmann, P. G. and Wajchenburg, B. L. (1999) Overnight lowering of free fatty acids with Acipimox improves insulin resistance and glucose tolerance in obese diabetic and nondiabetic subjects. Diabetes **48**, 1836–1841
30 Boden, G., Lebed, B., Schatz, M., Homko, C. and Lemieux, S. (2001) Effect of acute changes of plasma free fatty acids on intramyocellular fat content and insulin resistance in healthy subjects. Diabetes **50**, 1612–1617
31 Dey, D., Mukherjee, M., Basu, D., Datta, M., Roy, S. S., Bandyopadhyay, A. and Bhattacharya, S. (2005) Inhibition of insulin receptor gene expression and insulin signaling by fatty acid: interplay of PKC isoforms therein. Cell. Physiol. Biochem. **16**, 217–228
32 Kopp, E. and Ghosh, S. (1994) Inhibition of NF-κB by sodium salicylate and aspirin. Science **265**, 956–959
33 Yuan, M., Konstantopoulos, N., Lee, J., Hansen, L., Li, Z. W., Karin, M. and Shoelson, S. E. (2001) Reversal of obesity and diet-induced insulin resistance with salicylates or targeted disruption of IKKβ. Science **293**, 1673–1677

Received 8 March 2010/7 May 2010; accepted 18 May 2010
Published as BJ Immediate Publication 18 May 2010, doi:10.1042/BJ20100330

Biochem. J. (2010) **429**, 451–462 (Printed in Great Britain) doi:10.1042/BJ20100330

online data

SUPPLEMENTARY ONLINE DATA

NF-κB mediates lipid-induced fetuin-A expression in hepatocytes that impairs adipocyte function effecting insulin resistance

Suman DASGUPTA*[1], Sushmita BHATTACHARYA*[1], Anindita BISWAS*, Subeer S. MAJUMDAR†, Satinath MUKHOPADHYAY‡, Sukanta RAY‡ and Samir BHATTACHARYA*[2]

*Cellular and Molecular Endocrinology Laboratory, Department of Zoology, School of Life Science, Visva-Bharati (A Central University), Santiniketan 731235, India, †Division of Cellular Endocrinology, National Institute of Immunology, Aruna Asaf Ali Marg, New Delhi 110067, India, and ‡Department of Endocrinology and Metabolism, I.P.G.M. E&R/S.S.K.M. Hospital, Kolkata 700020, India

MATERIALS AND METHODS

Free Ca^{2+} ($[Ca^{2+}]_i$) measurements

$[Ca^{2+}]_i$ was estimated by following the method described by Kenny et al. [1] except for the variation of $CaCl_2$ concentrations in the incubation buffer. The Fura-2 fluorescence of cells was recorded using a Shimadzu dual-excitation-wavelength spectrofluorimeter with excitation at 340 and 380 nm and emission at 500 nm. Fura-2 fluorescence increased with the increasing $[Ca^{2+}]_i$, changes in fluorescence intensity reflected the changes in $[Ca^{2+}]_i$ concentrations.

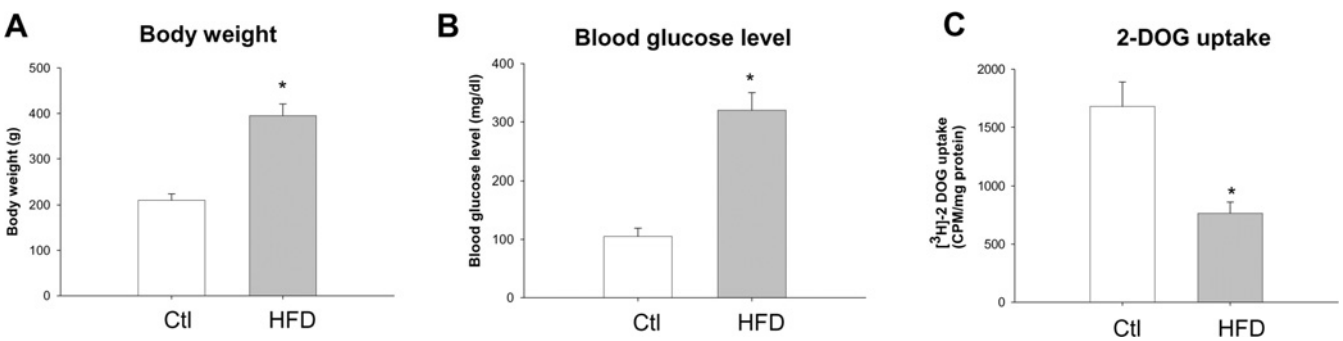

Figure S1 Insulin resistance in HFD-fed rats

(**A**) Adult rats were fed on a normal diet (Ctl) or on an HFD for 12 weeks. Comparison of body weight of normal and HFD rats. (**B**) Blood glucose levels of normal and HFD rats was measured using the glucose oxidase method. (**C**) Skeletal muscle cells isolated from control and HFD-fed rats were incubated *in vitro* with [^{3}H]2-DOG followed by the determination of its uptake. Means ± S.E.M. were calculated from six independent experiments. *$P < 0.001$, compared with Ctl.

[1] These authors contributed equally to this work.
[2] To whom correspondence should be addressed (email bhattacharyasa@gmail.com).

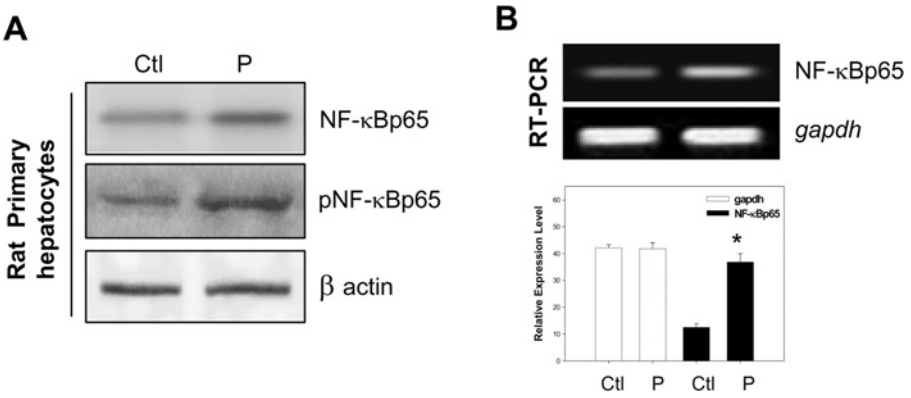

Figure S2 Palmitate stimulates NF-κB in rat primary hepatocytes

(**A**) Rat primary hepatocytes were incubated without (Ctl) or with (P) palmitate for 4 h. Cells were lysed and immunoblotted with anti-NF-κBp65 or anti-pNF-κBp65 antibodies. β-Actin served as an internal control. (**B**) RNA extracted from these incubations was subjected to RT–PCR and real-time PCR using NF-κB-specific primers where *Gapdh* served as an internal control. Means $\pm$ S.E.M. were calculated from three independent experiments. *P<0.001, compared with Ctl.

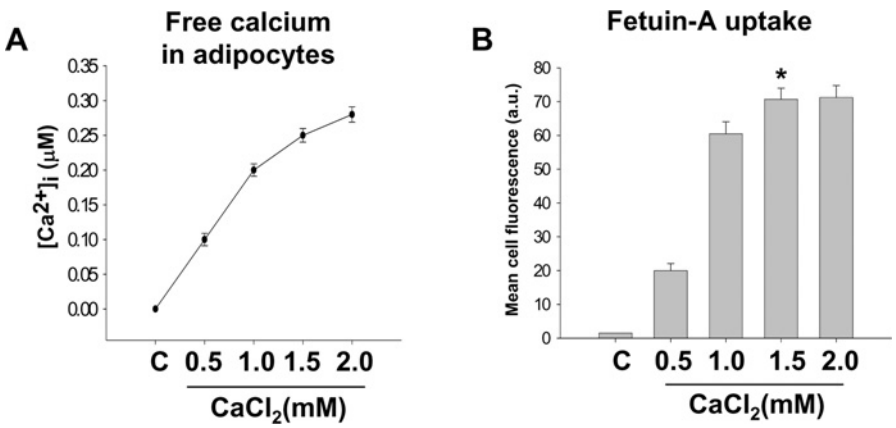

Figure S3 Effects of Ca^{2+} on fetuin-A uptake by 3T3-L1 adipocytes

(**A**) 3T3-L1 adipocytes were incubated with Fura-2 in Tris-balanced salt solution containing various concentrations of $CaCl_2$ (0.5, 1.0, 1.5 and 2.0 mM), and free Ca^{2+} was measured using a spectrofluorimeter. (**B**) 3T3-L1 adipocytes were incubated with FITC-conjugated fetuin-A in the absence or presence of various concentrations of $CaCl_2$ (0.5, 1.0, 1.5 and 2.0 mM). Cells were then washed thoroughly and lysed, and the supernatant was used to quantify the amount of internalized FITC-labelled fetuin-A using the spectrofluorimeter. Means $\pm$ S.E.M. were calculated from three independent experiments. *P<0.01 for 1.5 mM $CaCl_2$ compared with C (control). a.u., arbitrary units.

Table S1 The putative NF-κB-binding sites on the pFetA-luc vector

Putative NF-κB-response elements on the fetuin-A promoter region of pFetA-luc vector and representative of the same in classical NF-κB. The position of six putative elements is given with respect to the transcription start site.

Putative elements	Position	Sequence
N1	−251/−242	5′-GGGGCAGGGA-3′
N2	−277/−268	5′-TGGTCATTTC-3′
N3	−395/−386	5′-TTGGCATCTC-3′
N4	−559/−568	5′-ATTTCCTCTG-3′
N5	−794/−785	5′-AAGCAGAAAT-3′
N6	−957/−948	5′-ATGAAGTCCC-3′
Classical NF-κB response element		5′-GGGRNNYYCC-3′

REFERENCE

1 Kenny, J. S., Kisaalita, W. S., Rowland, G., Thai, C. and Foutz, T. (1997) Quantitative study of calcium uptake by tumorigenic bone (TE-85) and neuroblastoma X glioma (NG108-15) cells exposed to extremely-low-frequency (ELF) electric fields. FEBS Lett. **414**, 343–348

Received 8 March 2010/7 May 2010; accepted 18 May 2010
Published as BJ Immediate Publication 18 May 2010, doi:10.1042/BJ20100330